https://ntrs.nasa.gov/search.jsp?R=19650002848 2018-07-26T04:20:11+00:00Z

NASA CONTRACTOR REPORT

NASA CR-140

NASA CR-140

GPO PRICE $ _____

OTS PRICE(S) $ 1.50

Hard copy (HC) _____

Microfiche (MF) .75

FACILITY FORM 602

N65 [illegible] 9

(ACCESSION NUMBER) (THRU)

58 1

(PAGES) (CODE)

CR-140 32

(NASA CR OR TMX OR AD NUMBER) (CATEGORY)

FRACTURE TESTING OF WELDMENTS

by J. A. Kies, H. L. Smith,
H. E. Romine, and H. Bernstein

Prepared *by*
NAVAL RESEARCH LABORATORY
Washington D. C.
for

NATIONAL AERONAUTICS AND SPACE ADMINISTRATION • WASHINGTON, D. C. • DECEMBER 1964

NASA CR-140

FRACTURE TESTING OF WELDMENTS

By J. A. Kies, H. L. Smith, H. E. Romine, and H. Bernstein

Distribution of this report is provided in the interest of information exchange. Responsibility for the contents resides in the author or organization that prepared it.

Prepared by
NAVAL RESEARCH LABORATORY
Washington, D. C.

for

NATIONAL AERONAUTICS AND SPACE ADMINISTRATION

For sale by the Office of Technical Services, Department of Commerce,
Washington, D.C. 20230 -- Price $1.50

FRACTURE TESTING OF WELDMENTS

by

J. A. Kies*, H. L. Smith*, H. E. Romine**, and H. Bernstein***

Synopsis

12449

A new and improved apparatus has been designed and built for three point loading of bend bars. A new formula for K_{Ic} independent of Young's modulus has been derived which fits experimental calibrations and calculations by B. Gross with satisfactory accuracy. A formula is provided by which the requirements for specimen size and notch depth can be calculated for measuring K_{Ic} for a given yield strength of material. A number of comparisons are shown for the effect of rolling direction on K_{Ic} for base plate and for several different kinds of welding. The effect of notch position on K_{Ic} is shown. The slow bend test has advantages of adaptability and simplicity for the purpose at hand.

It seems noteworthy that the effect of directionality on K_{Ic} in the base plate is in the same direction but magnified in tests of the welds in the 250 Ksi yield strength grade. For some welding procedures the K_{Ic} for some positions in welds was better than for the base plate with no deficiency of hardness. Significance tests were applied to the differences between average values of K_{Ic}. From the K_{Ic} numbers listed one may calculate the larges tolerable surface crack corresponding to a given stress applied. The center of the weld presents the lowest toughness of any position.

Author

*U. S. Naval Research Laboratory, Washington, D. C. 20390
**U. S. Naval Weapons Laboratory, Dahlgren, Virginia
***Special Projects Office, BuWeps, Navy Dept., Washington, D. C.

TABLE CONTENTS

	Page
Synopsis	iii
Introduction	1
The Bend Specimen and Testing Fixtures	2
Formulas and Calibration	2
Plastic Zone Limitations	6
Demonstration of Linearity between K_{Ic} and Nominal Fiber Stress	6
Limitations on Specimen Size and Notch Depth	7
Comparison of Plane Strain Fracture Toughness by the Slow Bend Test and by the Single Edge Notch Test	8
Material and K_{Ic} Test Results for Base Plate	10
Tungsten Inert Gas Welds	15
Metal Inert Gas Welds	19
Short Arc Welds	21
Summary of K_{Ic} Test Results	23
Conclusions	27
Acknowledgements	29
References	30
List of Figures	31
APPENDIX	
Failure Analysis Example - Weld Flaw	49
Choice of Specimen Type (3 point bend test)	53
Use of K Values Computed from an Equation	54

FRACTURE TESTING OF WELDMENTS

by

J. A. Kies[1], H. L. Smith[1], H. E. Romine[2], and H. Bernstein[3]

Introduction

Techniques for measuring the fracture toughness of weldments are not unique or different from those for testing base plate except for simple considerations of adequate sampling and for studying metallurgical variables not present in the base plate. In this investigation use of $\mathscr{G}_{Ic}$ (or K_{Ic}) toughness numbers was helpful because, from current evidence, these numbers do not vary significantly with specimen geometry. Thus the specimens could be efficiently planned from an expense viewpoint. The present paper contains a description of a bend test procedure and neglects others only because our immediate concern is with steels for large solid propellant booster rockets in which the yield strength and the plate thicknesses are both high enough to make the use of bend tests convenient. A list of the detailed reasons for choosing the 3 point loading bend test for the immediate purposes is given in the Appendix. For other applications other tests might be preferred. In choosing a specimen for a given task in measuring fracture toughness, a few simple rules should be observed as follows:

(a) The plastic zone size at critical load should be small compared with the crack depth and with the unbroken ligament.

(b) The computed nominal stress disregarding stress concentration factor should not exceed 1.1 times the nominal tensile yield strength.

---

(1) U. S. Naval Research Laboratory, Washington, D. C. 20390
(2) U. S. Naval Weapons Laboratory, Dahlgren, Virginia
(3) Special Projects Office, BuWeps, Navy Dept., Washington, D. C.

(c) The machined notch should be terminated or extended by a real crack, most conveniently a fatigue crack.

(d) Testing arrangements should provide reproducible load deflection relations not disturbed by variable warpage in the specimen or insecure seating of the test fixture.

(e) A closed formula for K is highly desirable.

The Bend Specimen and Testing Fixtures

The bend specimen chosen for convenience in testing the plate is shown in Fig. 1. The test fixturing was especially designed to provide self-alignment and security from tilting during load application. Figure 2 shows an assembly of specimen and fixture in the testing machine. Further details are to be found in Ref. (1)

In order to satisfy testing condition (d) above, a considerable effort was expended to provide a stable fixture easily lending itself to alignment and proper centering. Details of parts for the bend test apparatus are shown in Fig. 3 and sliding guides for axially centering of the test bar are shown in Fig. 4.

Special attachments were made for use in fatiguing the notched bars so as to introduce a real crack. Figure 5 shows two assembly views of the fatigue apparatus and the test specimen. Figure 6 shows the construction of the special lever arm used for gripping the specimen.

Formulas and Calibration

In general if we can measure loads and deflections with sufficient accuracy we can write for P total load and A total crack area:

$$\mathcal{G} = \frac{P^2}{2} \frac{d\,(1/M)}{dA} \qquad (1)$$

where $1/M$ is the compliance such that the elastic deflection δ is

$$\delta = \frac{P}{M}$$

Here we wish to consider bend bars of width B and depth D. Then

$$\mathscr{G} = \frac{P^2}{2} \frac{d\,(1/M)}{B\,da} , \tag{1a}$$

where "a" is crack depth. If we choose to normalize with respect to plate thickness, we can write

$$\mathscr{G} = \frac{1}{2} \left(\frac{P}{B}\right)^2 \frac{d\,(B/M)}{da} \tag{1b}$$

Mast has postulated (Ref. 2) that for the Irwin $\mathscr{G}$ factors $\mathscr{G}_p$ and $\mathscr{G}_m$ (strain energy release rates) acting independently on a crack and due to tensile and bending loads, the total $\mathscr{G}$ is

$$\mathscr{G} = \mathscr{G}_p + \mathscr{G}_m \quad . \tag{2}$$

In this case the total K or stress intensity factor is not obtained by stress analysis but is given by

$$K_I^2 = \frac{E}{(1 - \nu^2)} \left(\mathscr{G}_{Ip} + \mathscr{G}_{Im}\right)$$

for plain strain. From the experimental point of view the derivatives of the compliance with respect to crack size would have to be independent for Eq. (2) to be correct. In case these are not independent then the total stress due to all loads would be obtained and the resulting total K or stress intensity factor determined accordingly. There would be no point in determining K_p and K_m separately. If $\mathscr{G}_p$ and $\mathscr{G}_m$ are not independent then K_p and K_m would have no usefulness as separate quantities.

In the present paper $\mathscr{G}_p = 0$ for the bend bars and there is no ambiguity.

Mast (2) obtained approximate expressions for K_p and K_m for deep notches. His expression for K_m is

$$K_m = \frac{2\ Pe}{B\sqrt{\pi}\ \ell^{3/2}} \tag{3}$$

where Pe is the bending moment "m" on the unbroken ligament

$$K_m = \frac{2\ m}{B\sqrt{\pi}\ \ell^{3/2}}$$

and

$$\mathscr{G}_I = \frac{(1 - \nu^2)}{E} \quad \frac{4\ m^2}{B^2\ \pi\ \ell^3} \tag{4}$$

For 3 point loading as used in our experiments

$$m = \frac{PL}{4}$$

and

$$\mathscr{G}_I = \frac{1}{2}\left(\frac{P}{B}\right)^2 \frac{(1 - \nu^2)\ L^2}{2\ E\ \pi\ \ell^3} \tag{4a}$$

$$\frac{d\ (B/M)}{da} = \frac{(1 - \nu^2)\ L^2}{2\ E\ \pi\ \ell^3} \tag{5}$$

However, simple dimensional considerations permit us to adapt this to shallow as well as deep notches by rewriting (5) as

$$\frac{d\ (B/M)}{da} = \frac{(1 - \nu^2)\ L^2}{2\ \pi\ E}\left[\frac{1}{\ell^3} - \frac{\ell^3}{(D/2)^6}\right] \tag{6}$$

$$a + 2\ell = D \qquad da = -\ 2\ d\ell$$

$$\alpha = 2\ell/D \qquad D\ d\alpha = -\ da$$

The second term within the bracket of Eq. (6) assures that $\mathscr{G} = 0$ for $a = 0$ without changing the dimensions of the bracket. The choice of exponent 3 on ℓ^3 was made to correspond with calibration data of Romine and the calculations of B. Gross (Ref. 4) except that for the Irwin calibration the second term, $\frac{\ell}{(D/2)^4}$, a first power correction, provided a much better fit. D is the total beam depth. Equation (6) may be re-

written as (7) with the insertion of a factor S needed to include the 1.2 Irwin factor for surface notches (Ref. 3) and other effects.

$$\frac{d\,(B/M)}{da} = \frac{4\,S\,(1 - \nu^2)\,L^2}{\pi\,E\,D^3}\left[\frac{1}{\alpha^3} - \alpha^3\right] \tag{7}$$

and

$$\frac{B}{M} = \frac{2\,S\,(1 - \nu^2)\,L^2}{\pi\,E\,D^2}\left[\frac{1}{\alpha^2} + \frac{\alpha^4}{2}\right] + \text{Const.} \tag{8}$$

Then

$$\mathcal{G}_I = 2\left(\frac{P}{B}\right)^2 \frac{S\,(1 - \nu^2)\,L^2}{\pi\,E\,D^3}\left[\frac{1}{\alpha^3} - \alpha^3\right] \tag{9}$$

Since

$$\mathcal{G}_I = \frac{1}{2}\left(\frac{P}{B}\right)^2 \frac{d\,(B/M)}{da}$$

then for $L = 2L_1$ and $S = 1.667$

$$R = \frac{K_I\,D^{3/2}}{P/B\,L_1} = 2.060\left\{\frac{1}{\alpha^3} - \alpha^3\right\}^{1/2} \tag{10}$$

The selection of $S = 1.667$ was done for the purpose of fitting the Romine and other calibration data as shown in Fig. 7. This figure also shows that Equation (10) fits the values of R as calculated by B. Gross (Ref. 4) well within experimental uncertainties in calibrations.* Equation (10) is the same for symmetrical four point bending except that L_1 then is the distance between outer and next inner load points. We have no experimental data at present for checking Equation (10) for four point loading. In obtaining R experimental for the Romine calibration bars 2-3 and 2-6 the values of $E = 27 \times 10^6$ psi, $\nu = 0.25$, $D = 0.750$ inch, and $L_1 = 3$ inches were used. For purposes of entering the Romine data on Fig. 7,

$$R = 0.824\sqrt{\frac{d\,(B/M)}{da}} \times 10^3\,,$$

where $\frac{d\,(B/M)}{da}$ was experimentally determined.

---

*Good agreement between Equation (10) and a corrected version of a formula by Beuchner (7) has also been reported in a private communication by Mr. Carl Hartbower, Aerojet-General Corp.

Plastic Zone Limitations

Thus far Equations (9, 10) for $\mathscr{G}_I$ and K_I do not include plastic zone corrections. Introduction of this correction complicates the formula considerably and it is suggested that this is not necessary provided that the nominal fiber stress at the root of the notch is kept below 1.1 times the yield stress. The estimated plane strain plastic zone size, $2\ r_y$, when $\sigma_{nom} = 1.1\ \sigma_{YS}$ is about 0.04". Use of the plasticity correction would at the extreme increase K by about 10%.

Demonstration of Linearity between K_{Ic} and Nominal Fiber Stress

A demonstration of the necessary linearity between K_{Ic} (for fixed span and approximately fixed notch dimensions) and nominal fiber stress may be seen in Fig. 8a. These data points are for maraging steel bars from a heat different from that for the bulk of this report. Only specimens containing surface notches are shown. $\mathscr{G}_{Ic}$ values were computed using an equation based upon a compliance calibration. K_{Ic} values were then computed from the equation

$$K_{Ic}^2\ (1 - \nu^2) = E\ \mathscr{G}_{Ic} \quad . \tag{11}$$

If one computes K_{Ic} using Equation (10) for these data points, the relationship between K_{Ic} and the load P is:

$$K_{Ic} = 27.95\ P \tag{12}$$

If the load is converted to maximum fiber stress at the notch root, S', and dividing by the yield strength of the material, the expression for K_{Ic} becomes

$$K_{Ic} = 93{,}175 \left(\frac{S'}{\sigma_{YS}} \right) \tag{13}$$

The straight line through the origin representing this equation in Fig. 8a shows good agreement with Romine's results. Part of the scatter shown by the

open squares may be expected on the basis of microstructural variability in welds; however, the rest of the data shows the required linearity. Variations in S'/σ_{YS} for a given K_{Ic} value reflect variations in notch depth. Variations larger than 10 Ksi $\sqrt{in.}$ in the K_{Ic} values reflect real changes in toughness. Within a fixed type of material (base metal, for example) the K_{Ic} toughness variations are believed to be due to delaminations. Romine's data for plate surface notched specimens range in notch depth only from 0.10 to 0.14 inches. Within this range no special correlation of K_{Ic} with notch depth was observed.

Limitations on Specimen Size and Notch Depth

In forecasting the required specimen size and notch depth, it is necessary to know in advance how high K_{Ic} will be.

Assuming that at the root of the notch the nominal fiber stress is

$$\sigma_{nom} = \frac{m\,\ell}{I} \tag{14}$$

$$\sigma_{nom} = 3\,\frac{P\,L_1}{B\,\alpha^2\,D^2} \tag{15}$$

Then

$$K_I = \sigma_{nom}\sqrt{D}\;0.687\left\{\alpha - \alpha^7\right\}^{1/2} \tag{16}$$

If the upper limit of validity is for $\sigma_{nom} = 1.1\,\sigma_{YS}$

$$K_{I\ lim} = 0.756\,\sigma_{YS}\sqrt{D}\left\{\alpha - \alpha^7\right\}^{1/2} \tag{17}$$

For the limiting case $K_{Ic} = K_{Ic\ lim}$

$$\Delta a_{lim} \cong \frac{K^2_{Ic\ lim}}{4\sqrt{2}\,\sigma^2_{YS}}$$

or

$$\Delta a_{lim} = 0.101\ D \left\{ \alpha - \alpha^7 \right\} \tag{18}$$

$f_2(\alpha) = \left\{ \alpha - \alpha^7 \right\}$ has a maximum at $a/D = 0.28$ or $\alpha = 0.72$. Thus the most favorable notch depth ratio is about 0.28. However, the term $(\alpha - \alpha^7)$ changes by only 0.2% in going from an a/D value of 0.25 to a value of 0.30. So within this range of notch depth ratios one may simple use the equation

$$K_I = 0.540\ \sigma_{nom} \sqrt{D} \tag{19}$$

Comparison of Plane Strain Fracture Toughness by the Slow Bend Test and by the Single Edge Notch Test

Tests were made on 18 Ni (250,000 psi strength level) maraging steel plates from 3/4" thick, air melted stock. The bend tests were made with 3 point loading using 3/4" x 3/4" x 7.5" specimens while the single-edge-notch specimens were 3" x 12" x 0.75" in size loaded in tension with pin holes at W/2 position. Results are given in Table I (Ref. 5). The material used in this comparison was previously received from an outside source different from the one for which the bulk of the data are presented in this paper.

TABLE I

Comparison of Edge Notch Tear Tests with Bend Tests

	K_{Ic} From Compliance Bend Test (Ksi $\sqrt{in.}$)	K_{Ic} Eq. (10) (Ksi $\sqrt{in.}$)	K_{Ic} Single Edge Notch (Ksi $\sqrt{in.}$)	
Bar 2	79	81.2	82	Source B Steel
Bar 3	80	81.5	81	
	Av. 79.5	Av. 81.3	Av. 81.5	

TABLE I (Cont.)

Bend Bar Bar No.	⊥ or ‖	K_{Ic} Eq. (10) (Ksi $\sqrt{in.}$)	Spec. No. Edge Notch Tear	⊥ or ‖	K_{Ic} (Ksi $\sqrt{in.}$)
	Plate 1			Plate 2	
1-31-2	⊥	67.5	VII BA-2	⊥	73.0
1-31-3	⊥	67.2	VII BA-3	⊥	72.0
1-31-4	⊥	66.1	VII BA-4	⊥	69.0
1-31-5	⊥	68.8			
		Av. 67.4			Av. 71.3
	Plate 2			Plate 1	
2-31-2	‖	68.8	VII AA-2	‖	72.0
2-31-3	‖	67.0	VII AA-3	‖	75.0
2-31-4	‖	68.5			Av. 73.5
2-31-5	‖	68.3			
		Av. 68.1			

Earlier work by the U. S. Steel Corporation (Ref. 6) on 0.16" thick 18 Ni maraging steel of the 280,000 psi yield strength level gave the results shown in Table II. The single edge notch specimens were loaded in tension with the pin holes at w/3 position. $K_{Ic} = E\,\mathcal{G}_{Ic}/(1 - \nu^2)$ where $E = 27 \times 10^6$ psi and $\nu = 0.3$. The bend test values shown here are based on analytical results obtained by B. M. Wundt from work by Bueckner (Ref. 7).

TABLE II

Comparison of Edge Notch Tear Tests and Bend Tests

(U. S. Steel Co. Tests)

K_{Ic} 3" Wide Central-Notch (Ksi $\sqrt{in.}$)	K_{Ic} Single Edge Notch (Ksi $\sqrt{in.}$)	K_{Ic} Eq. (10) (Ksi $\sqrt{in.}$)	K_{Ic} Bend Test by Bueckner Formula (Ksi $\sqrt{in.}$)
77.0	77.0	85.0	82.5
	79.8	83.8	82.5
	Av. 78.4	Av. 84.4	Av. 82.5

It is tentatively concluded from Tables I and II that K_{Ic} obtained in bend tests using Equation (10) gives good agreement with single edge pop-in tests. Further testing is in progress.

Material and K_{Ic} Test Results for 3/4-inch Thick Plate of 18 Percent Nickel Maraging Steel shown in Tables III et. seq.

Compositions and heat numbers are shown in Table III for materials tested and results shown in Tables IV to XIII inclusive.

TABLE III-a

Materials Compositions

Composition	Plates Heat X14636	Plates Heat X53013
C	0.03	0.02
Mn	0.06	0.02
P	0.005	0.006
S	0.010	0.009
Si	0.10	0.04
Ni	18.37	17.59
Mo	4.70	4.80
Co	8.49	8.06
Ti	0.42	0.49
Al	0.13	0.07
Cu		0.12

TABLE III-b

Mechanical Properties of the Plates

	Heat X14636	Heat X53013
Aged Properties (915°F - 4 hours)		
Hardness R_c	50-53	
0.2% Offset Yield	263 Ksi ‖	
	248 " ⊥	
Ult. Tensile Strength	272 Ksi ‖	
	259 " ⊥	
Elong. in 2 inches, %	4.0 ‖	
	4.6 ⊥	
Reduction Area, %	30 ‖	
	33 ⊥	
Annealed (1550°F - 1 hour)		
Hardness	32.8 R_c	32.3 R_c

TABLE III-c

Weld Rod Chemistry

C	0.02%	Mo	4.62%
Si	0.02%	Al	0.09%
Mn	0.03%	Ti	0.45%
S	0.005%	H_2	1.5 ppm
P	0.004%	O_2	14.0 ppm
Ni	18.24%	N_2	25.0 ppm
Co	7.90%		

Note: Identical weld rod chemistry for TIG, MIG, and Short Arc Welding. Weld rod drawn to different diameters.

TABLE III-d

Correspondence Between Plate and Heat Numbers, Weld Method, and Rolling Direction

NRL Plate No.	Weld Method	Plate No. (U. S. Steel Co.)	Heat No. (U. S. Steel Co.)	Rolling Direction Orientation	
				Weld Bead	Bar Length
1	TIG	42298	X14636	⊥	‖
2	TIG	42298	X14636	‖	⊥
5	MIG	42298	X14636	⊥	‖
6	MIG	156872	X53013	‖	⊥
11	Short Arc	156872	X53013	⊥	‖

Details of the welding procedures are supplied by Excelco Developments Inc. and are included in the Appendix along with NRL chemical analyses of weld metal taken from test bars.

Table IV shows K_{Ic} values obtained on base plate using bars cut perpendicular to and parallel with the rolling direction. Conditions are 3 point bending. K_{Ic} is computed from Equation (10) and visual notch depth.

It is noteworthy that all of the tests in Table IV were made with the notch on the plate surface so as to simulate expected cracking in rocket cases. This direction is conducive to crack arrest by delamination or diversion of fracture path. The dependence of K_{Ic} on direction of crack propagation has been previously investigated by Romine (Ref. 5). Average K_{Ic} for plate surface notches was reported as 83 Ksi $\sqrt{in.}$ versus 69 Ksi $\sqrt{in.}$ for edgewise propagation in base bars cut in the rolling direction in the earlier tests. For bars cut transverse to the rolling direction the effect was in the same direction but less pronounced; average K_{Ic} values were 66 and 64 Ksi $\sqrt{in.}$ respectively for the same plate.

Typical fracture appearances for bend bars in which the notches are on the plate surface and plate edge are shown in Figs. 9 and 10 for plates from two different sources not represented in Tables IV - XIII. It is clear that the orientation of the notch has an influence on the toughness of the base plates. Similar differences according to crack propagation direction are illustrated for NRL plate 2 in Figs. 11 and 12.

TABLE IV

NRL Plates 1 and 2

K_{Ic} Values for Base Plate Equation (10) and Visual Notch Depth "a" Used

Plate 1 Bars ⊥ to Rolling Direction, Base Plate			Plate 2 Bars ‖ to Rolling Direction, Base Plate		
Bar No.	"a", in.	K_{Ic} (Ksi $\sqrt{in.}$)	Bar No.	"a", in.	K_{Ic} (Ksi $\sqrt{in.}$)
1-1	0.16	83.7	2-1	0.06	87.2
1-2	0.15	78.1	2-2	0.05	79.2
1-3	0.14	79.7	2-3	Calib.	
1-4	0.12	74.1	2-4	0.07	79.5
1-5	0.14	93.1	2-5	0.05	9.15
1-6	0.15	69.5	2-6	Calib.	
1-7	0.15	80.1	2-7	0.06	84.7
1-8	0.14	76.2	2-8	0.05	82.2
1-9	0.13	74.2	2-9	Ultrasonic Test	
1-10	0.14	73.1	2-10	0.05	87.3
1-11	0.13	77.0	2-11	0.07	88.0
1-12	0.15	79.6	2-12	0.05	84.9
1-13	0.13	72.6	2-13	Calib.	
1-14	0.14	75.8	2-14	0.07	81.5
1-15 }	Calib.		2-15	0.08	88.5
1-16 }			2-16	0.07	89.5
1-17	0.15	75.3	2-17	0.07	84.8
1-18	0.14	75.5	2-18	0.08	79.8
1-19	0.14	82.2	Edge Fract.		
1-20	0.14	76.9	2-20	0.20	85.0
1-21	0.13	77.9	2-21	0.16	84.9
1-22	0.14	76.1	2-22	0.17	86.3
1-23	Calib.		2-23	0.15	88.0
1-24	Calib.		2-24	0.15	82.2
1-25	0.13	73.3	2-25	0.07	80.7
1-26	0.15	71.9	2-26	Calib.	
1-27	0.14	79.9	2-27	0.05	75.4
1-28	0.13	76.2	2-28	0.14	87.2
1-29	0.13	75.7	2-29	0.05	81.1
1-30	0.13	73.5	2-30	0.07	84.7
	Av.	77.0		Av.	84.3

TABLE V

K_{Ic} Numbers for Notches in the Center of TIG Welds

Welds are run transverse to the bars.

Bar Lengths ⊥ Plate 2 to Rolling Direction			Bar Lengths ‖ Plate 1 with Rolling Direction		
Bar No.	Visual "a", in.	K_{Ic} (Ksi $\sqrt{in.}$)	Bar No.	Visual "a", in.	K_{Ic} (Ksi $\sqrt{in.}$)
IV BA-1	0.17	66.9	IV AA-1	0.15	88.8
2	0.13	57.2	2	0.13	80.1
3	0.16	70.6	3	0.16	87.5
4	0.15	61.0	4	0.15	91.2
5	0.17	68.7	5	0.16	103.1
6	0.18	57.8	6	0.14	93.3
7	0.14	60.3	7	0.20	113.8
8	0.15	67.6	8	0.15	90.3
9	0.14	79.5	9	0.16	69.8
10	0.14	68.0	10	0.15	74.5
11	0.16	77.0	11	0.15	60.3
12	0.15	82.4	12	0.15	85.7
13	0.18	80.2	13	0.15	74.2
14	0.14	59.4	14	0.15	80.9
15	0.16	81.0	15	0.15	75.9
16	0.15	75.3	16	0.16	64.1
17	0.16	68.2	17	0.18	91.0
18	0.16	72.3			
	Av.	69.6		Av.	83.8
	c.v.	0.12		c.v.	0.15

Note: The large difference between K_{Ic} for bars IV AA-7 and IV AA-11 was attributable to microstructure. Bar-7 was fine grained and Bar-11 coarse grained at the root of the starting crack. This will receive more future detailed study by metallography.

Tungsten Inert Gas Welds

Tungsten inert gas welding was investigated. The typical sequence of passes is indicated by an etched cross section shown in Fig. 13. K_{Ic} values for plates TIG welded are given in Tables V to VIII. The orientation of the bars perpendicular and parallel with rolling direction is indicated. The weld beads were transverse to the bars and the position of the notch is coded as follows:

C.W. - center of the weld
F.Z. - fusion zone where base plate is melted
H.A.Z. - heat affected zone in the base plate
D.B. - dark band just outside H.A.Z.

The typical TIG weld lay-up and the positions of the notches are shown in Fig. 13a. The weld bead lay-ups for MIG and short arc welds are shown on etched bend bars in Figs. 13b and 13c respectively.

The K_{Ic} results for the fusion zone or edge of the fusion zone in TIG welds are shown in Table VI. Each specimen was etched on the sides prior to testing to verify the position of the bottom of the fatigue crack below the notch. Although some uncertainty remained, the position code was assigned in accordance with the etched appearance not always the same as the original intended position. The code letters assigned were in accordance with Fig. 14. The notch position assignments were the best that could be done on this basis and within the authors' ability to distinguish etched structures with the usual visual aids. In order to get valid K_{Ic} numbers, say for F.Z. or H.A.Z., it is not necessary for the propagation to proceed more than a very small distance in the specified structure. The load at initiation of the fracture is hopefully the only load recorded. The pop-in must produce an offset of at least 1/16-inch on the record which corresponds to 0.0004-inch deflection of the specimen. This corresponds to an increment in crack depth of 0.004-inch. The records indicate that the load at pop-in is never appreciably different from that after this amount of pop-in.

The center-of-weld toughness was found to be less than that at any other position.

The microstructural details existing at the tips of the cracks were not investigated. This will be the subject of a future investigation aimed at offering guidance for future materials improvement.

TABLE VI

K_{Ic} for the Fusion Zone TIG Welds

Bar Lengths ⊥ Plate 2 to Rolling Direction			Bar Lengths ‖ Plate 1 with Rolling Direction		
Bar No.	Visual "a", in.	K_{Ic} (Ksi $\sqrt{in.}$)	Bar No.	Visual "a", in.	K_{Ic} (Ksi $\sqrt{in.}$)
IV BD-4	0.15	77.3	IV AD-1		
5	0.15	87.0	2	Calibration bars	
6	0.15	76.2	3		
7	0.19	82.3	4	0.19	106.7
8	0.15	89.6	5	0.16	97.3
9	0.15	81.7	6	0.17	100.8
IV BB-18	0.17	80.5	7	0.19	109.3
	Av.	82.1	8	0.15	90.0
	c.v.	0.06	9	0.16	103.9
			10	0.16	92.0
				Av.	100.0
				c.v.	0.07

The K_{Ic} test results for the heat affected zone (H.A.Z.) are shown in Table VII for TIG welds.

TABLE VII

K_{Ic} for the Heat Affected Zone TIG Welds (H.A.Z.)

Bar Lengths ⊥ Plate 2 to Rolling Direction			Bar Lengths ‖ Plate 1 with Rolling Direction		
Bar No.	Visual "a", in.	K_{Ic} (Ksi $\sqrt{in.}$)	Bar No.	Visual "a", in.	K_{Ic} (Ksi$\sqrt{in.}$)
IV BB-8	0.18	87.6	IV AB-9	0.14	101.9
9	0.18	66.8	10	0.14	88.6
10	0.17	71.1	11	0.14	82.3
11	0.15	59.5	12	0.14	82.3
12	0.19	73.2	13	0.15	104.0
13	0.14	90.0	14	0.14	102.7
14	0.19	60.7	17	0.16	103.1
15	0.15	76.3	18	0.16	91.6
16	0.15	85.8			
17	0.17	75.9			
	Av.	74.7		Av.	94.6
	c.v.	0.14		c.v.	0.10

The K_{Ic} test results for dark band at the junction of the base plate and heat affected zone are given in Table VIII for TIG welds.

TABLE VIII

K_{Ic} for the Dark Band at the Junction of Base Plate and Heat Affected Zone TIG Welds (D.B.)

Bar Lengths ⊥ Plate 2 to Rolling Direction			Bar Lengths ‖ Plate 1 with Rolling Direction		
Bar No.	Visual "a", in.	K_{Ic} (Ksi $\sqrt{in.}$)	Bar No.	Visual "a", in.	K_{Ic} (Ksi $\sqrt{in.}$)
IV BB-1	0.15	62.3	IV AB-1	0.15	90.3
2	0.17	62.0	2	0.13	99.8
3	0.16	59.8	3	0.17	117.0
4	0.16	63.5	4	0.13	82.6
5	0.15	76.5	5	0.14	97.9
6	0.13	72.1	6	0.13	106.4
7	0.16	71.8	7	0.16	83.0
	Av.	66.9	8	0.15	102.2
	c.v.	0.09	19	0.14	95.1
			20	0.15	91.9
				Av.	96.6
				c.v.	0.10

Metal Inert Gas Welds

A photograph showing the etched cross section of a typical MIG weld is shown as Fig. 13b. Toughness numbers for such welds notched in the center of the weld are given in Table IX.

TABLE IX

K_{Ic} for MIG Welds Notched in the Center of the Weld (C.W.)

Bar Lengths ⊥ NRL Plate 6 to Rolling Direction			Bar Lengths ‖ NRL Plate 5 with Rolling Direction		
Bar No.	Visual "a", in.	K_{Ic} (Ksi √in.)	Bar No.	Visual "a", in.	K_{Ic} (Ksi √in.)
II BA-1	0.15	70.2	II AA-1	0.14	72.0
2	0.15	74.1	4	0.13	71.8
3	0.15	62.6	6	0.13	70.7
4	0.20	54.4	7	0.14	64.4
5	0.14	70.5	8	0.13	85.9
6	0.15	63.2	10	0.12	71.4
7	0.14	70.6	11	0.12	75.8
8	0.14	71.8	13	0.15	80.1
9	0.15	67.0	15	0.14	60.4
10	0.13	87.3	16	0.13	71.4
11	0.14	74.1	17	0.13	102.7
12	0.13	86.9	18	0.14	105.7
13	0.15	84.4		Av.	77.7
14	0.14	83.0			
15	0.15	81.8			
16	0.14	78.8			
17	0.13	85.3			
18	0.14	74.3			
19	0.13	71.4			
	Ave.	74.3			
	c.v.	0.12			

K_{Ic} results for notches terminating in the heat affected zone of MIG welds are shown in Table X.

TABLE X

Toughness in the Heat Affected Zone MIG Welds (H.A.Z.)

Bar Lengths ⊥ NRL Plate 6 to Rolling Direction			Bar Lengths ‖ NRL Plate 5 with Rolling Direction		
Bar No.	Visual "a", in.	K_{Ic} (Ksi $\sqrt{in.}$)	Bar No.	Visual "a", in.	K_{Ic} (Ksi $\sqrt{in.}$)
II BB-2	0.13	90.8	II AB-1	0.15	85.0
3	0.15	91.8	3	0.12	87.4
4	0.14	93.2	4	0.13	92.6
5	0.13	89.8	6	0.11	105.1
6	0.13	102.3	7	0.13	105.7
7	0.14	93.4	8	0.15	78.4
		Av. 93.6	9	0.16	81.6
		c.v. 0.10	10	0.16	86.7
			11	0.14	99.0
					Av. 91.3
					c.v. 0.10

K_{Ic} test results for notches terminating in the center of the weld and heat affected zones for Short Arc Welds are shown in Tables XI and XII respectively.

TABLE XI

Short Arc Weld Toughness Data for Center of the Weld

Bar Lengths ⊥ Plate 7 to Rolling Direction		
Bar No.	Visual "a", in.	K_{Ic} (Ksi $\sqrt{in.}$)
V BA-1	0.150	43.5
2	0.120	75.4
3	0.155	60.0
4	0.140	48.0
5	0.155	53.5
6	0.160	52.6
7	0.145	69.0
8	0.150	59.0
9	0.155	51.5
10	0.160	56.5
	Av.	56.9
	c.v.	0.16

Bar Lengths ‖ Plate 11 with Rolling Direction		
Bar No.	Visual "a", in.	K_{Ic} (Ksi $\sqrt{in.}$)
V AA-1	0.15	64.1
2	0.14	75.9
3	0.14	73.3
4	0.14	72.8
5	0.15	68.6
6	0.14	61.5
7	0.13	67.4
8	0.14	65.2
9	0.13	89.1
10	0.14	79.3
11	0.14	69.7
12	0.14	74.7
13	0.12	71.4
14	0.15	72.4
15	0.17	77.8
16	0.13	75.9
17	0.14	75.8
18	0.12	79.1
19	0.14	69.4
	Av.	72.8
	c.v.	0.09

TABLE XII

K_{Ic} Test Results for Notches Terminating in the Heat Affected Zone, Short Arc Welds

Bar Lengths ⊥ Plate 7 to Rolling Direction			Bar Lengths ‖ Plate 11 with Rolling Direction		
Bar No.	Visual "a", in.	K_{Ic} (Ksi $\sqrt{in.}$)	Bar No.	Visual "a", in.	K_{Ic} (Ksi $\sqrt{in.}$)
V BB-2	0.120	92.5	V AB-1	0.12	113.3
4	0.130	96.5	2	0.13	96.4
5	0.140	89.5	3	0.11	103.2
7	0.140	85.5	4	0.12	111.3
8	0.130	86.5	5	0.14	101.1
	Av.	90.1	6	0.14	101.1
	c.v.	0.04	7	0.14	120.4
			8	0.14	116.2
			9	0.14	116.9
			10	0.14	98.1
			11	0.15	109.9
			12	0.15	98.7
			13	0.14	102.4
			14	0.14	113.4
			15	0.14	106.8
			16	0.12	115.6
			17	0.13	104.5
			18	0.15	92.6
				Av.	106.8
				c.v.	0.07

Summary of the Test Results

The average K_{Ic} values and their coefficients of variation are shown for the different weld methods, bar orientations, and notch positions in Table XIII. The coefficients of variation are of about the same magnitude usually reported by other authors and for other test procedures. On this basis the bend test method is not appreciably better or worse than other tests such as the edge notch tear test. The significances of the differences between average K_{Ic} values are shown in Table XIV. The levels of significance are assigned on the basis of the probability function of (t) in the usual "t" test. P(T) is the probability that in another set of tests the average values being compared would overlap because of scatter in the results. Qualitative terms used in Table XIV are as follows for designating the differences between averages:

H.S. = Highly Significant,	P(t)	< 0.024
S. = Significant,	P(t)	0.025 to 0.074
Pr.S. = Probably significant,	P(t)	0.075 to 0.14
Po.S. = Possibly significant,	P(t)	0.15 to 0.25
N.S. = Not significant,	P(t)	> 0.26

TABLE XIII

Summary of K_{Ic} Average Values and Their Coefficient of Variation

Table No.	Orientation of Bar with Rolling Dir.	Kind of Weld	Location of Notch	K_{Ic} Average (Ksi $\sqrt{in.}$)	Coefficient of Variation	Heat No.
IV	⊥	Base Plate		76.96	0.060	X14636
IV	‖	Base Plate		84.33	0.041	X14636
V	⊥	T.I.G.	C.W.	69.63	0.116	X14636
V	‖	T.I.G.	C.W.	83.79	0.152	X14636
VI	⊥	T.I.G.	F.Z.	82.08	0.057	X14636
VI	‖	T.I.G.	F.Z.	100.00	0.068	X14636
VII	⊥	T.I.G.	H.A.Z.	74.69	0.139	X14636
VII	‖	T.I.G.	H.A.Z.	94.56	0.098	X14636
VIII	⊥	T.I.G.	D.B.	66.86	0.089	X14636
VIII	‖	T.I.G.	D.B.	96.62	0.104	X14636
IX	⊥	M.I.G.	C.W.	74.30	0.117	X53013
IX	‖	M.I.G.	C.W.	77.69	0.054	X14636
X	⊥	M.I.G.	H.A.Z.	93.55	0.101	X53013
X	‖	M.I.G.	H.A.Z.	91.28	0.104	X14636
XI	‖	Short Arc	C.W.	72.81	0.088	X53013
XII	‖	Short Arc	H.A.Z.	106.77	0.074	X53013

TABLE XIV-a

P(t) Values for Student's "t" Test of the Significance Between Mean K_{Ic} Values

Base Plate		TIG Welds									
		⊥				||					
⊥	||	C.W.	F.Z.	H.A.Z.	D.B.	C.W.	F.Z.	H.A.Z.	D.B.		
	<.01 H.S.	<.01 H.S.	.015 H.S.	>.3 N.S.	<.01 H.S.	- - - -	- - - -	- - - -	- - - -	⊥	Base Plate
		- - - -	- - - -	- - - -	- - - -	>.3 N.S.	<.01 H.S.	<.01 H.S.	<.01 H.S.	||	
			<.01 H.S.	.178 Po.S.	>.3 N.S.	<.01 H.S.	- - - -	- - - -	- - - -	C.W.	⊥ TIG
				.123 Pr.S.	<.01 H.S.	- - - -	<.01 H.S.	- - - -	- - - -	F.Z.	
					.107 Pr.S.	- - - -	- - - -	<.01 H.S.	- - - -	H.A.Z.	
						- - - -	- - - -	- - - -	<.01 H.S.	D.B.	
							<.01 H.S.	.07 S.	.016 H.S.	C.W.	|| Welds
								>.3 N.S.	>.3 N.S.	F.Z.	
									>.3 N.S.	H.A.Z.	

P(t) is the probability of a random variation in average K_{Ic} which would equal or exceed the difference shown between two average values of K_{Ic}.

H.S. =	Highly Significant,	P(t) <0.024
S. =	Significant,	P(t) 0.025 to 0.074
Pr.S. =	Probably Significant,	P(t) 0.075 to 0.14
Po.S. =	Possibly Significant,	P(t) 0.15 to 0.25
N.S. =	Not Significant,	P(t) >0.26

TABLE XIV-b

P(t) Values for Student's "t" Test of the Significance Between Mean K_{Ic} Values

MIG Welds				Short Arc Welds						
⊥		‖		⊥		‖				
C.W.	H.A.Z.	C.W.	H.A.Z.	C.W.	H.A.Z.	C.W.	H.A.Z.			
.21 Po.S.	< .01 H.S.	- - - -	- - - -	<.01 H.S.	<.01 H.S.	- - - -	- - - -		⊥	Base Plate
- - - -	- - - -	>.01 N.S.	.04 S.	- - - -	- - - -	<.01 H.S.	<.01 H.S.		‖	
.093 Pr.S.	<.01 H.S.	- - - -	- - - -	<.01 H.S.	<.01 H.S.	- - - -	- - - -	C.W.	⊥	TIG Welds
.05 S.	<.01 H.S.	- - - -	- - - -	<.01 H.S.	.014 H.S.	- - - -	- - - -	F.Z.		
>.3 N.S.	<.01 H.S.	- - -	- - - -	<.01 H.S.	<.01 H.S.	- - - -	- - - -	H.A.Z.		
.059 S.	<.01 H.S.	- - - -	- - - -	.032 S.	<.01 H.S.	- - - -	- - - -	D.B.		
- - - -	- - - -	.262 N.S.	.157 Po.S.	- - - -	- - - -	<.01 H.S.	<.01 H.S.	C.W.	‖	
- - - -	- - - -	<.01 H.S.	.074 S.	- - - -	- - - -	<.01 H.S.	.073 S.	F.Z.		
- - - -	- - - -	.015 H.S.	>.3 N.S.	- - - -	- - - -	<.01 H.S.	<.01 H.S.	H.A.Z.		
- - - -	- - - -	<.01 H.S.	.28 N.S.	- - - -	- - - -	<.01 H.S.	.026 S.	D.B.		
	<.01 H.S.	>.3 N.S.	- - - -	<.01 H.S.	<.01 H.S.	- - - -	- - - -	C.W.	⊥	MIG Welds
		- - - -	>.3 N.S.	<.01 H.S.	.24 Po.S.	- - - -	- - - -	H.A.Z.		
			.03 S.	- - - -	- - - -	.22 Po.S.	<.01 H.S.	C.W.	‖	
				- - - -	- - - -	<.01 H.S.	<.01 H.S.	H.A.Z.		
					<.01	<.01	- - - -	C.W.	⊥	Short Arc Welds
						- - - -	<.01 H.S.	H.A.Z.		
							<.01 H.S.	C.W.	‖	
								H.A.Z.		

Conclusions

1. K_{Ic} values from the bend tests agreed well with those from edge notched tear tests.
2. A new K_{Ic} closed formula for bend tests was obtained which is independent of Young's modulus of elasticity.
3. There were highly significant effects of rolling direction on K_{Ic} for both heats of the 250 grade steel.
4. For TIG welds in bars cut parallel with the rolling direction the average K_{Ic} values were higher by highly significant amounts than for bars cut perpendicular to the rolling direction. This was true for all four notch positions in the weld. The margins of superiority were magnified over that in the base plate. We have no explanation.
5. For MIG welds no comparison was available between directions perpendicular and parallel with the rolling direction.
6. For short arc welds the greatest average K_{Ic} was found in the heat affected zone. For the 250 Ksi yield strength steel the directionality effect in the base plate was reflected in the welds.
7. Where a comparison was available the TIG welds were more consistent and generally better than for the other types of welds investigated.
8. Where marked superiority of K_{Ic} for shallow (vs. deeper) notches in base plate was found, this could be explained on the basis of finer grain size and fewer carbide precipitates.

9. Where wide differences in K_{Ic} were found between different bars but in the center of the weld at equal depths, the difference correlated with microstructure. Coarse grained weld deposits with dendrites aligned mainly along the fracture path showed less toughness than fine dendrites randomly oriented.

Conclusions 8 and 9 are tentative and will be given additional study.

Acknowledgements

The authors are greatly indebted to the following:

Mr. R. G. Hayes and Mr. A. S. Jennings of the U. S. Naval Weapons Laboratory and Mr. W. E. Anderson of NRL for mechanical testing.

Mr. F. Stonesifer and Mr. Karl McKinney of NRL for calculations.

Mr. W. Cohen and Mr. N. Mayer of NASA Headquarters for the financial support of this research and testing program.

REFERENCES

1. Romine, H.E., "Plane Strain Fracture Toughness Measurements of Solid Booster Case Materials," U. S. Naval Weapons Laboratory Report No. 1884, 13 September 1963.

2. Mast, P., Private communication, not published.

3. Irwin, G.R., "The Crack Extension Force for a Crack at a Free Surface Boundary," NRL Report 5120, April 15, 1959.

4. Gross, B., Private communication.

5. Romine, H.E., "Plane Strain Fracture Toughness by the Slow Bend Test and Through-Thickness Tensile Properties of Unwelded 18 Ni (250) Maraging Steel Plate 3/4-inch Thick being Studied for use in Large Solid-Propellant Booster Rockets," NWL Report (to be published).

6. U. S. Steel Corp. letter of 11 Feb 1963 to Dr. J. M. Krafft.

7. Winne, D.H. and Wundt, B.M., "Application of the Griffith-Irwin Theory of Crack Propagation to the Bursting Behavior of Disks Including Analytical and Experimental Studies," ASME Paper No. 52A-249, presented December 1957.

LIST OF FIGURES

Fig. 1 - Bend test specimens

Fig. 2 - Assembly of bend test specimen and fixtures

Fig. 3 - Details of parts for bend test apparatus

Fig. 4 - Sliding guides for axially centering of test bar

Fig. 5 - Fatigue apparatus for introducing a crack at the bottom of the notch

Fig. 6 - Extension bar for fatigue machine

Fig. 7 - Equation (10) compared with experimental calibrations and calculations by B. Gross

Fig. 8a - Linearity between K_{Ic} and nominal stress

Fig. 8b - Linearity between K_{Ic} and nominal stress in other material

Fig. 9 - Effect of crack propagation direction on fracture appearance and K_{Ic}, Source A

Fig. 10 - Effect of crack propagation direction on fracture appearance and K_{Ic}, Source B

Fig. 11 - Appearance of crack propagation through the thickness and across the rolling direction NRL Plate 2

Fig. 12 - Appearance of crack propagation from an edge notch propagating across the rolling direction in NRL Plate 2

Fig. 13a - Etched bars showing TIG lay-up and position of notches in NRL Plate 2

Fig. 13b - Etched bars showing MIG lay-up and position of notches in NRL Plate 2

Fig. 13c - Etched bars showing short arc welds lay-up and position of notches in NRL Plate 2.

Fig. 14 - Cross section of weld area showing different locations of starting notch tipped with fatigue crack

Fig. A1 - Enlarged view of a fracture origin in a 156-inch diameter test chamber made of H-11 steel.

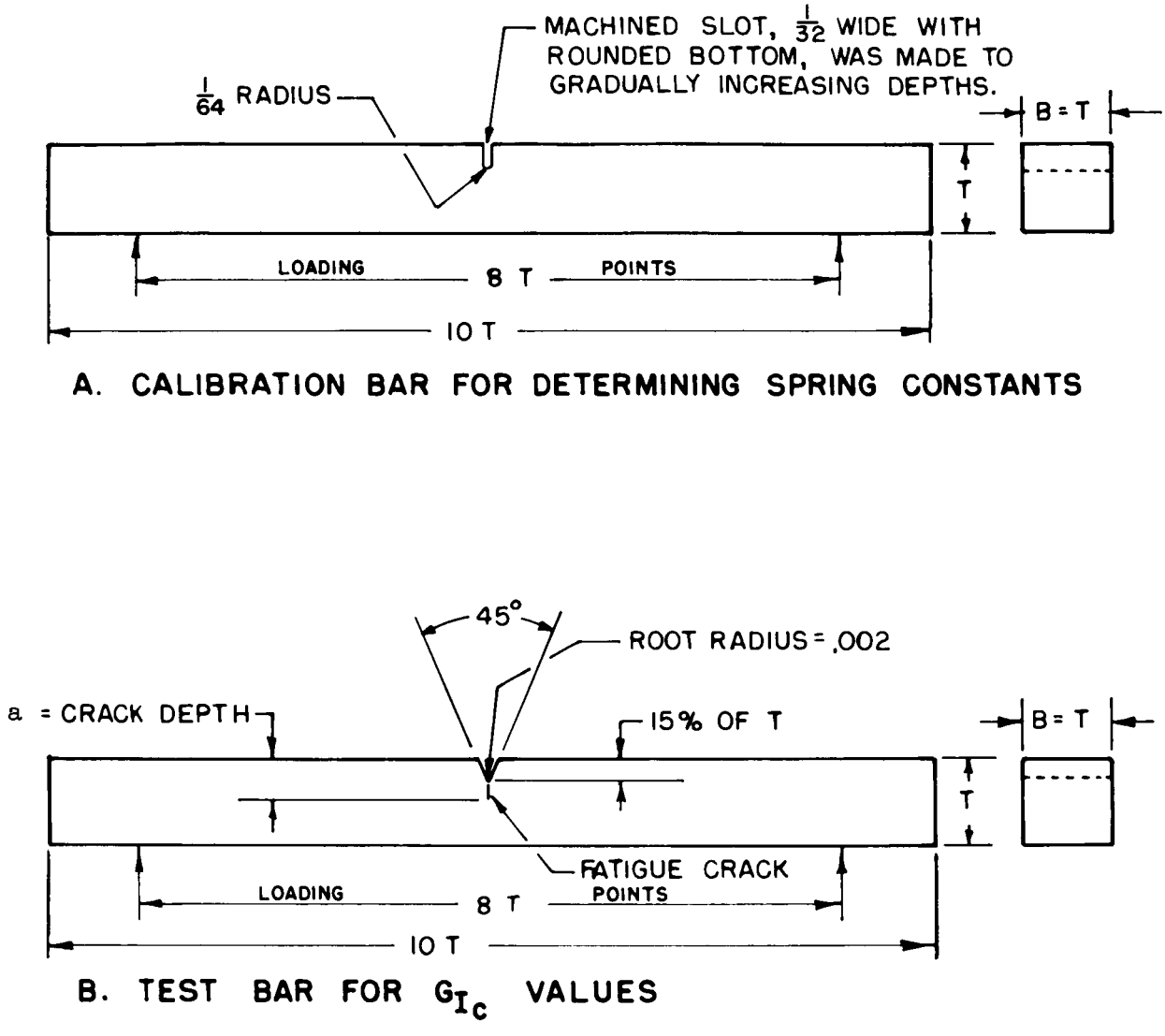

Figure 1.- Sketches of notched bar specimens.

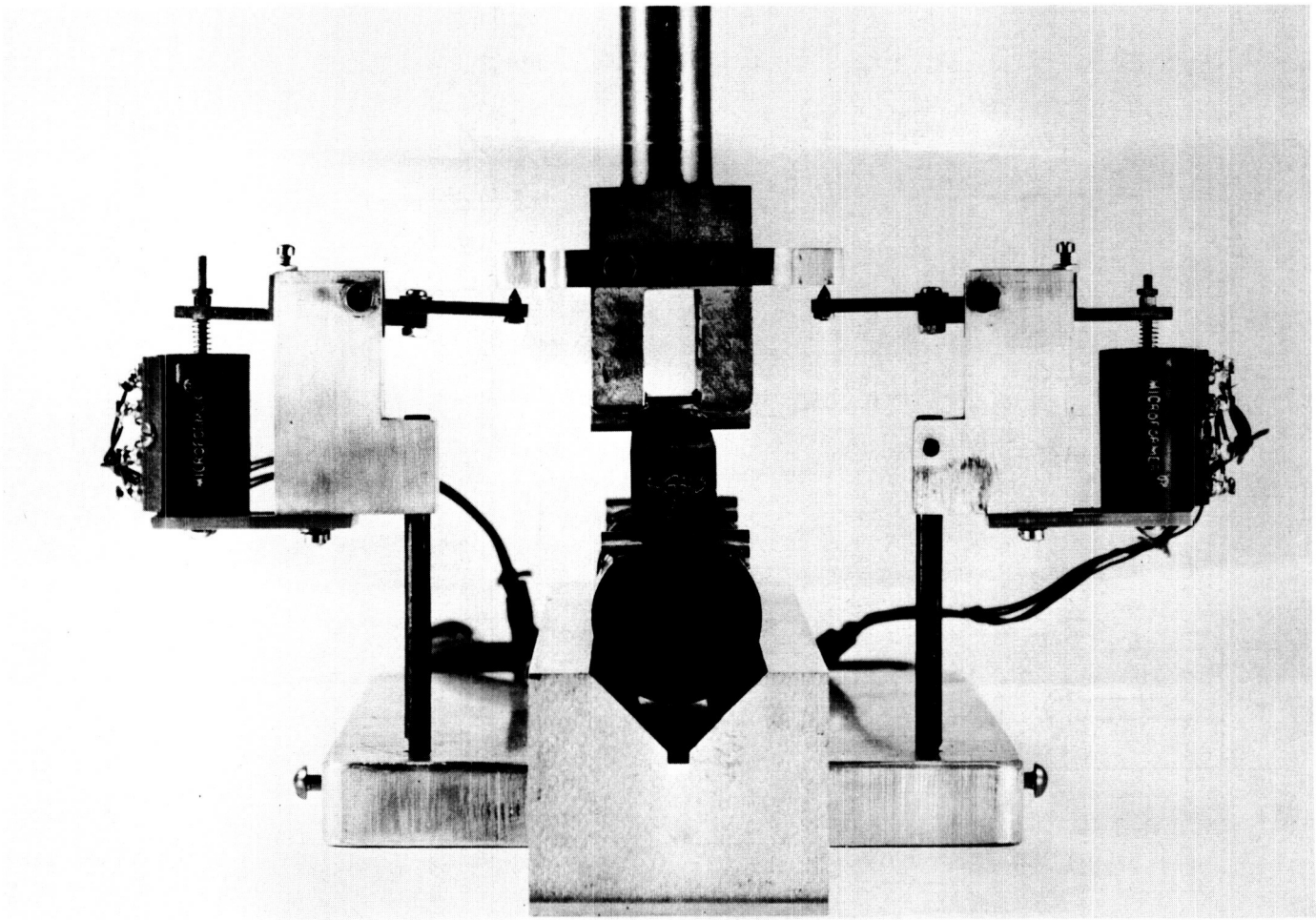

Figure 2.- End view of bend test apparatus showing transducers in position for measuring displacement of load. The transducers were adapted from a high-magnification averaging compressometer. Opening above upper loading point was intended for deflectometer arm formerly used to measure displacement.

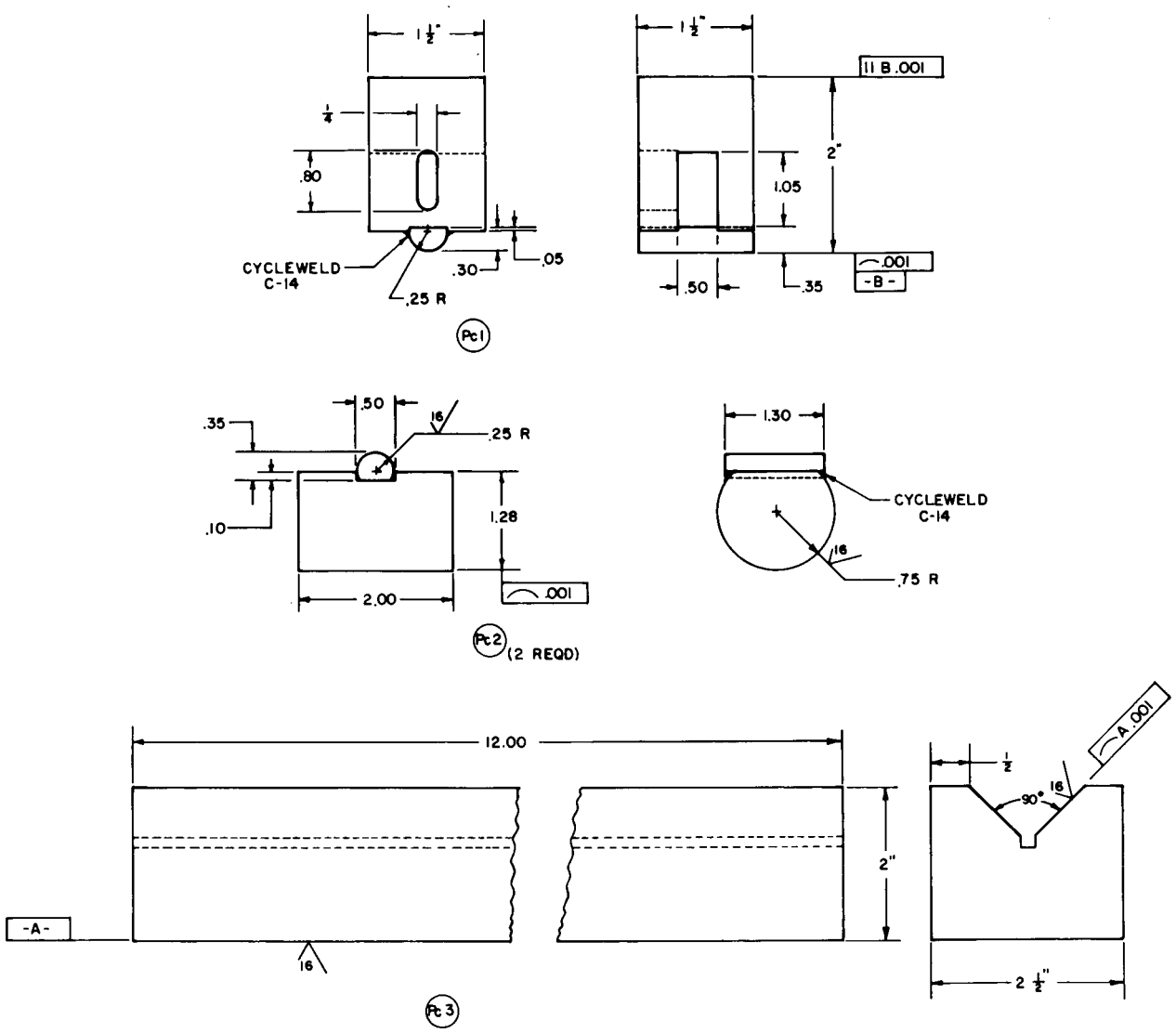

Figure 3.- Details of parts for bend test apparatus. The loading bars were 4340 steel hardened to 48 Rockwell C. The other parts were machined from quenched and tempered alloy steel with a hardness of about 26 Rockwell C (STS armor steel). Loading bars were cemented in place with Cycleweld C-14 adhesive (Chrysler Corp.) or equivalent.

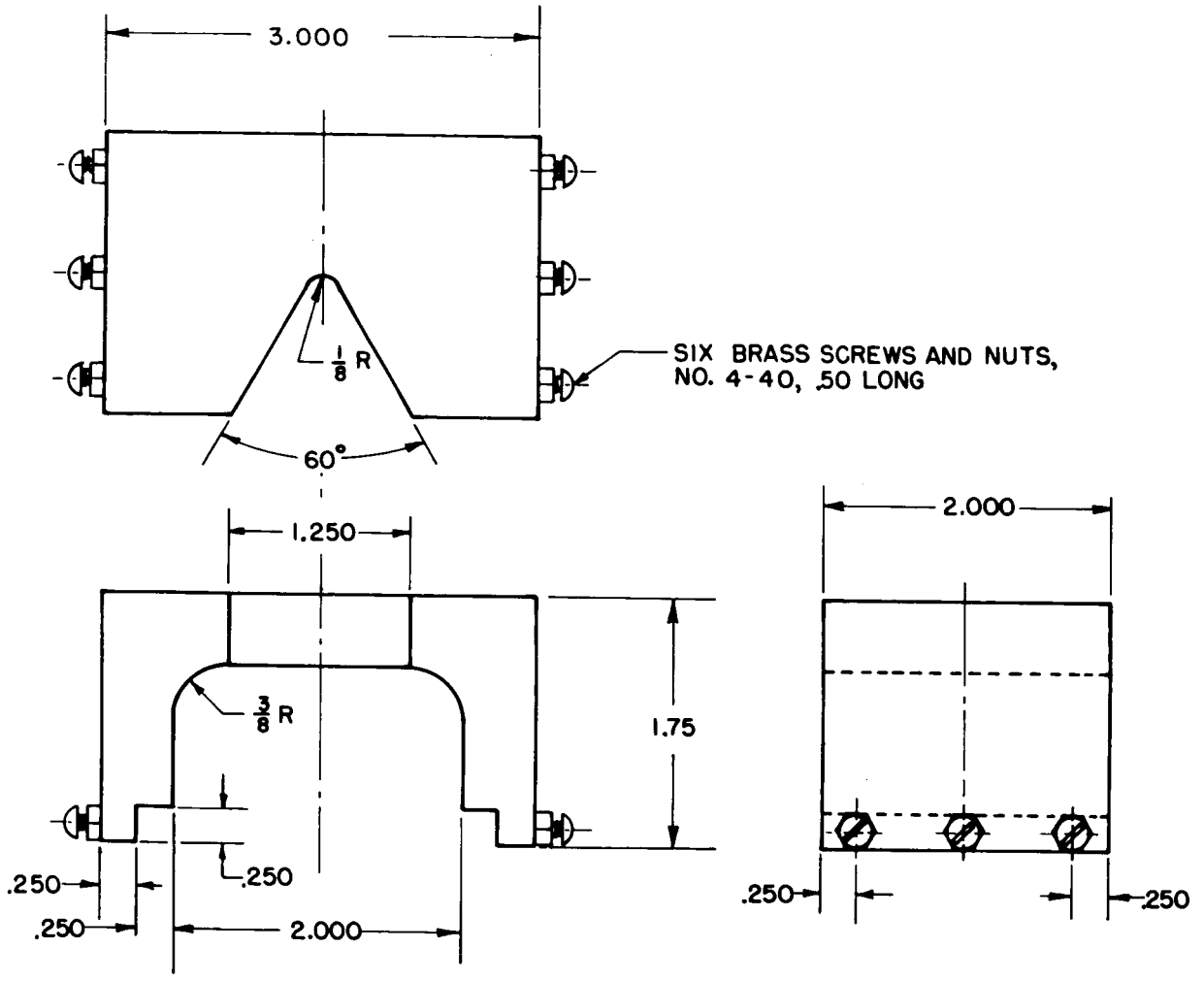

Figure 4.- Sliding guides for axial centering of test bar. Material: 2024-T4 aluminum alloy. Make two.

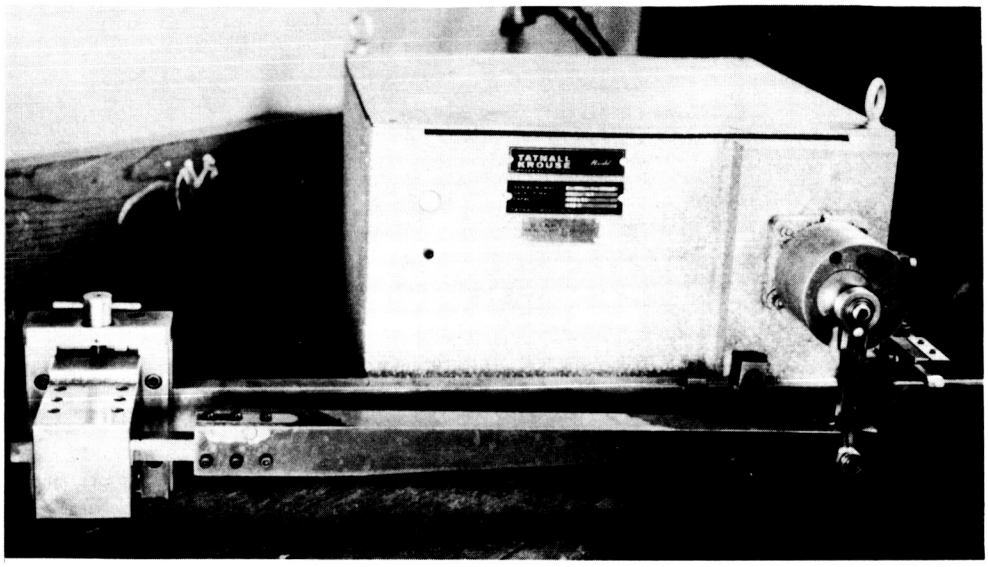

(A) Plate fatigue machine adapted to introduce fatigue crack at root of machined notch in bend test bars.

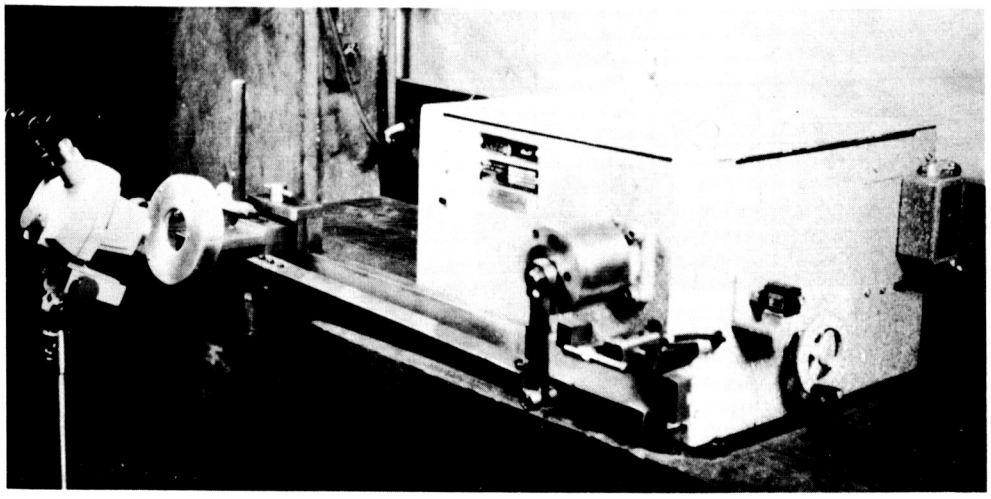

(B) Machine is stopped at intervals to inspect progress of fatigue crack. A zoom microscope and ring fluorescent light are shown in position to inspect front edge of crack. Microscope is racked in and a small first-surface mirror is held in position to inspect crack at back of notch.

Figure 5.- Fatigue machine for bend test bars.

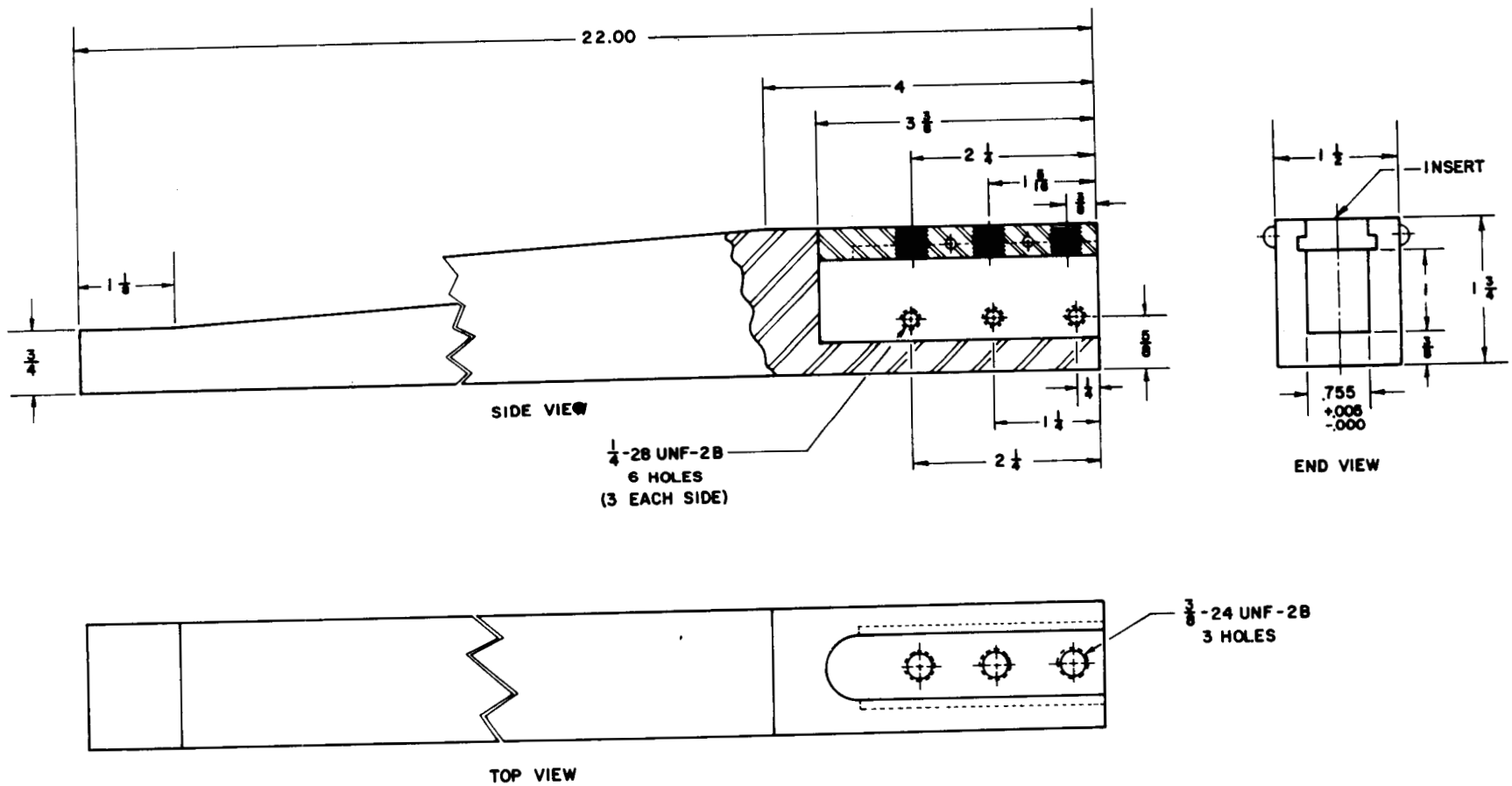

Figure 6.- Extension bar for fatigue machine. Material: steel, 4340.

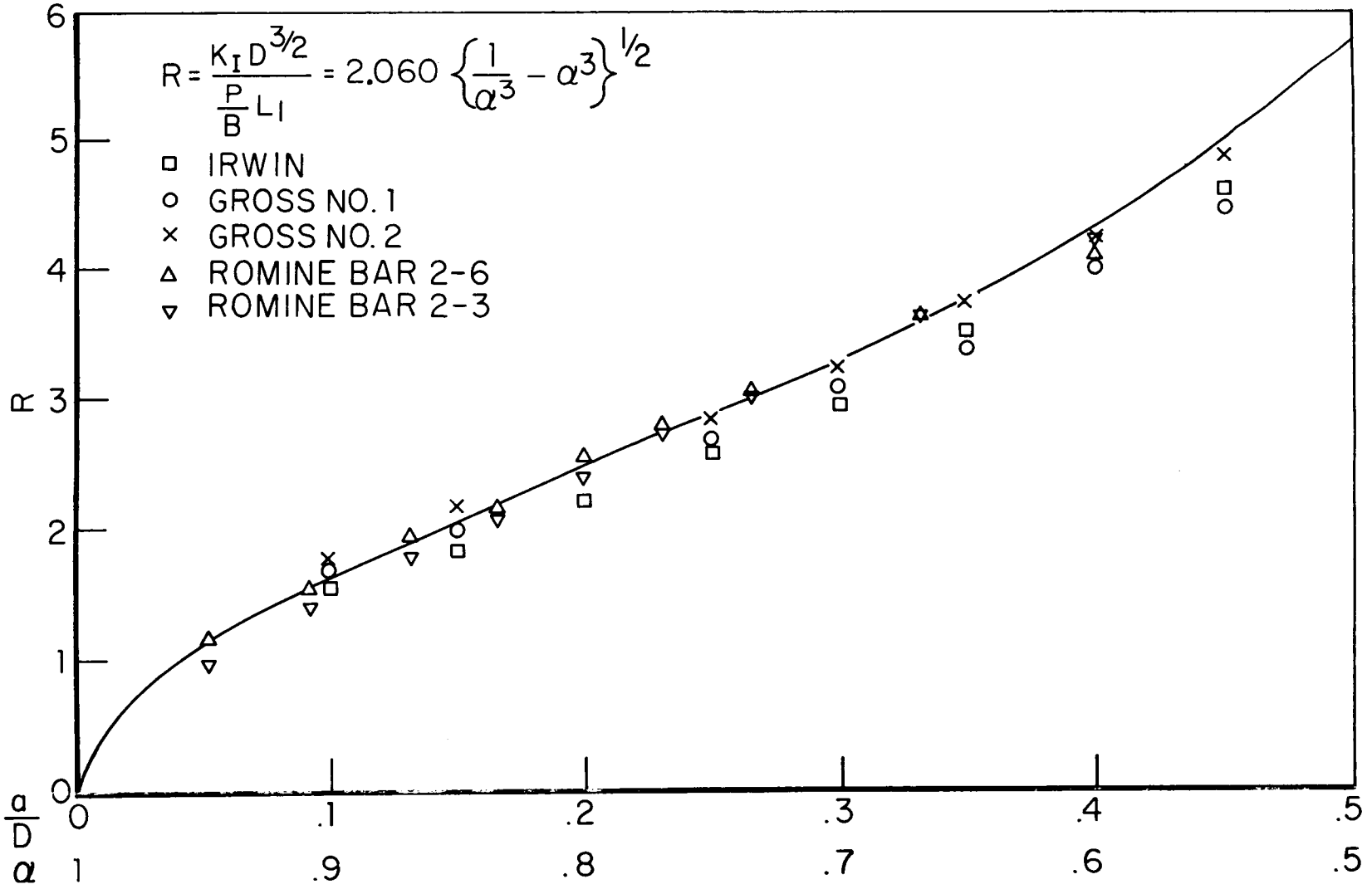
$R = \frac{K_I D^{3/2}}{\frac{P}{B} L_1} = 2.060 \left\{ \frac{1}{\alpha^3} - \alpha^3 \right\}^{1/2}$
IRWIN
GROSS NO. 1
GROSS NO. 2
ROMINE BAR 2-6
ROMINE BAR 2-3
R
0
1
2
3
4
5
6
a/D
0
.1
.2
.3
.4
.5
α
1
.9
.8
.7
.6
.5

Figure 7.

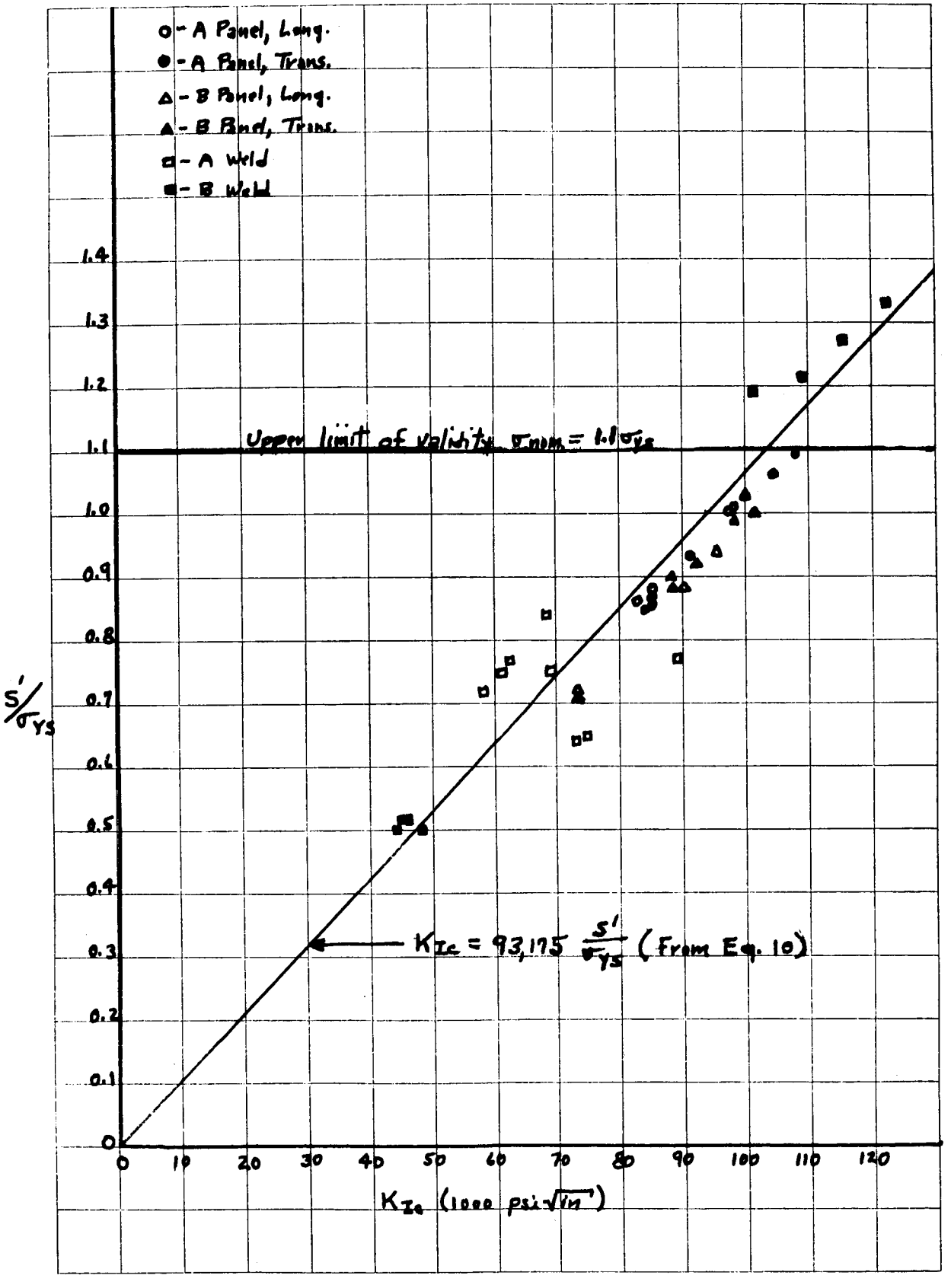
o - A Panel, Long.
● - A Panel, Trans.
Δ - B Panel, Long.
▲ - B Panel, Trans.
□ - A Weld
■ - B Weld
Upper limit of validity, σnom = 1.1 σys
S'/σYS
KIc = 93,175 S'/σYS (From Eq. 10)
KIc (1000 psi√in)
0
0.1
0.2
0.3
0.4
0.5
0.6
0.7
0.8
0.9
1.0
1.1
1.2
1.3
1.4
0
10
20
30
40
50
60
70
80
90
100
110
120

Figure 8a.

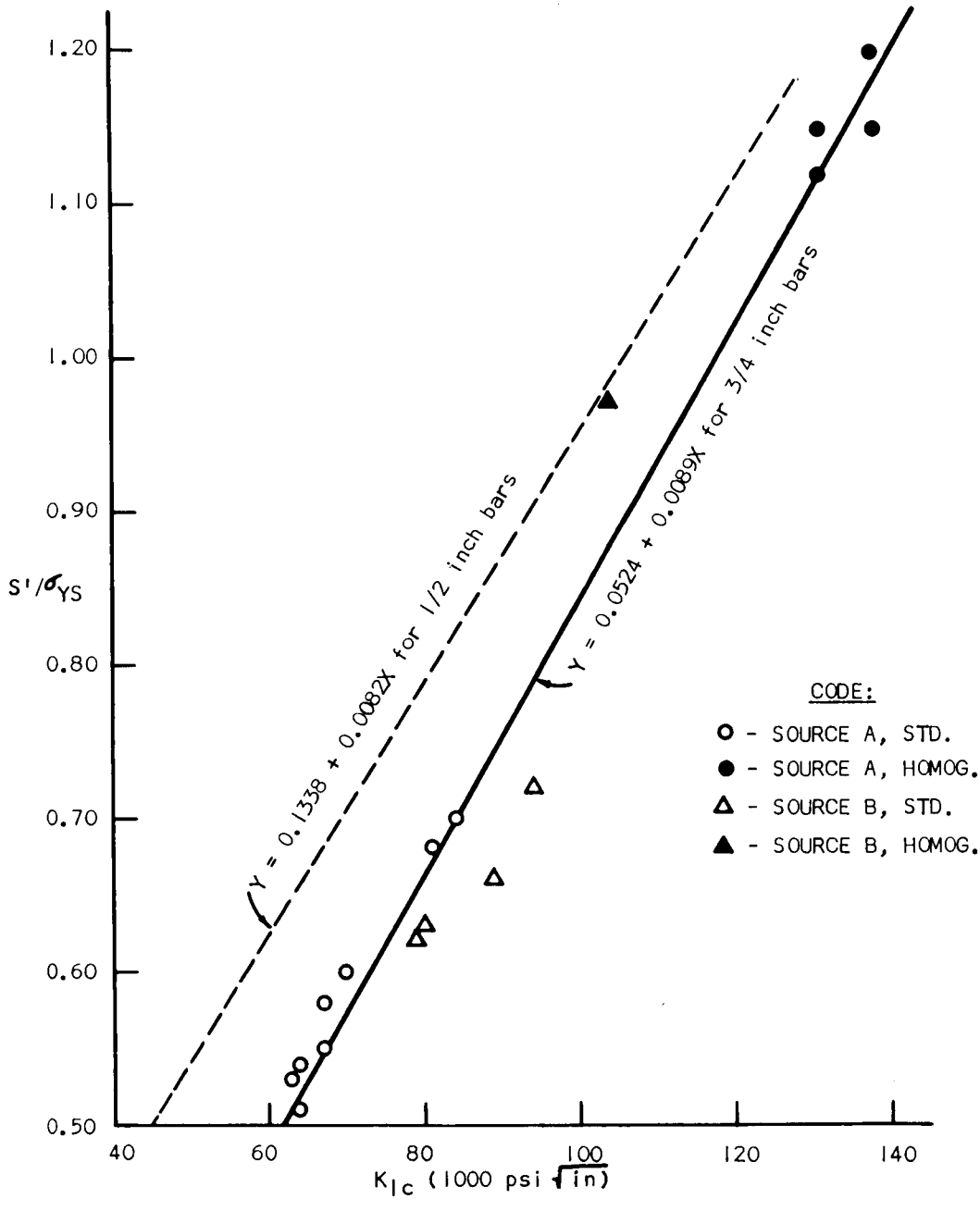

Figure 8b.- Correlation between ratio of maximum fiber stress to yield strength S'/σ_{YS} and fracture toughness K_{Ic}. Data points and solid line are for 3/4 inch bars in this report. The dashed line is a regression line for data on 1/2 inch bars from NWL report No. 1884. All K_{Ic} results were calculated from $\mathcal{G}_{Ic}$ by the relation: $K_{Ic}^2 = \frac{E\mathcal{G}_{Ic}}{(1 - \nu^2)}$. S' was calculated by the formula: $S' = \frac{6L}{4(d - a)^2}\left(\frac{P}{B}\right)$.

Avg. K_{Ic} - 66,000 psi $\sqrt{in}$

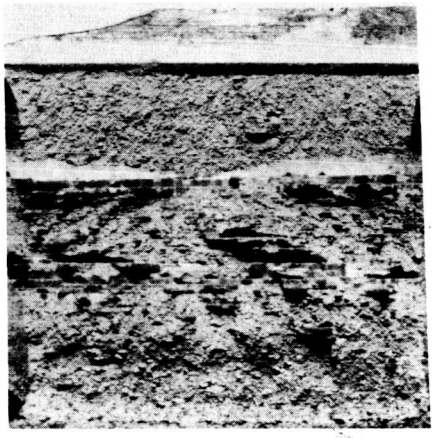

Avg. K_{Ic} - 83,000 psi $\sqrt{in}$

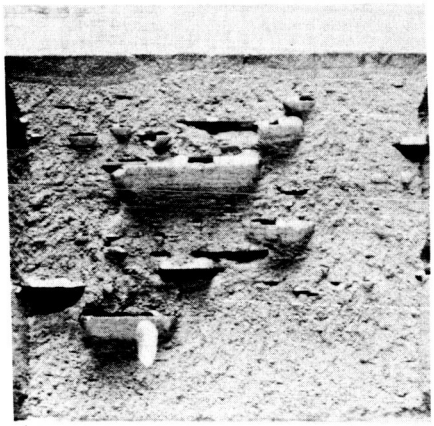

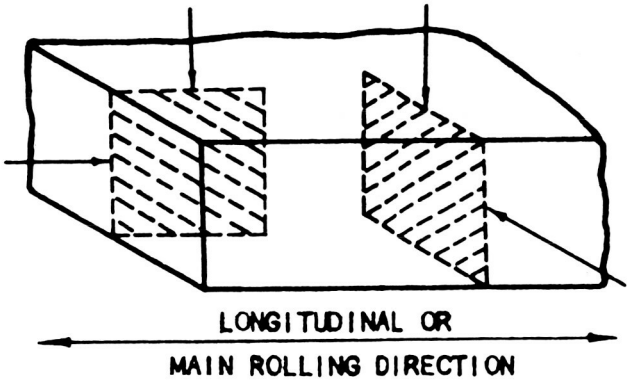

Small arrows indicate direction of crack propagation.

Avg. K_{Ic} - 64,000 psi $\sqrt{in}$

Avg. K_{Ic} - 69,000 psi $\sqrt{in}$

Figure 9.- Fracture appearance of slow-bend tests made to determine directional fracture toughness in 18 Ni (250) maraging steel plate 3/4 inch thick from source A. ×3.

Avg. K_{Ic} - 92,000 psi $\sqrt{in}$

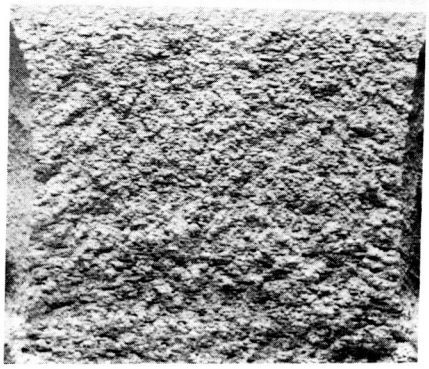

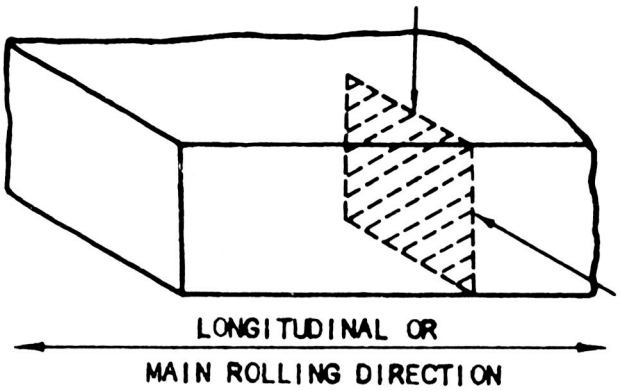

Small arrows indicate direction of crack propagation.

Avg. K_{Ic} - 80,000 psi $\sqrt{in}$

Figure 10.- Fracture appearance of slow-bend tests made to determine directional fracture toughness in 18 Ni (250) maraging steel plate 3/4 inch thick from source B. ×3.

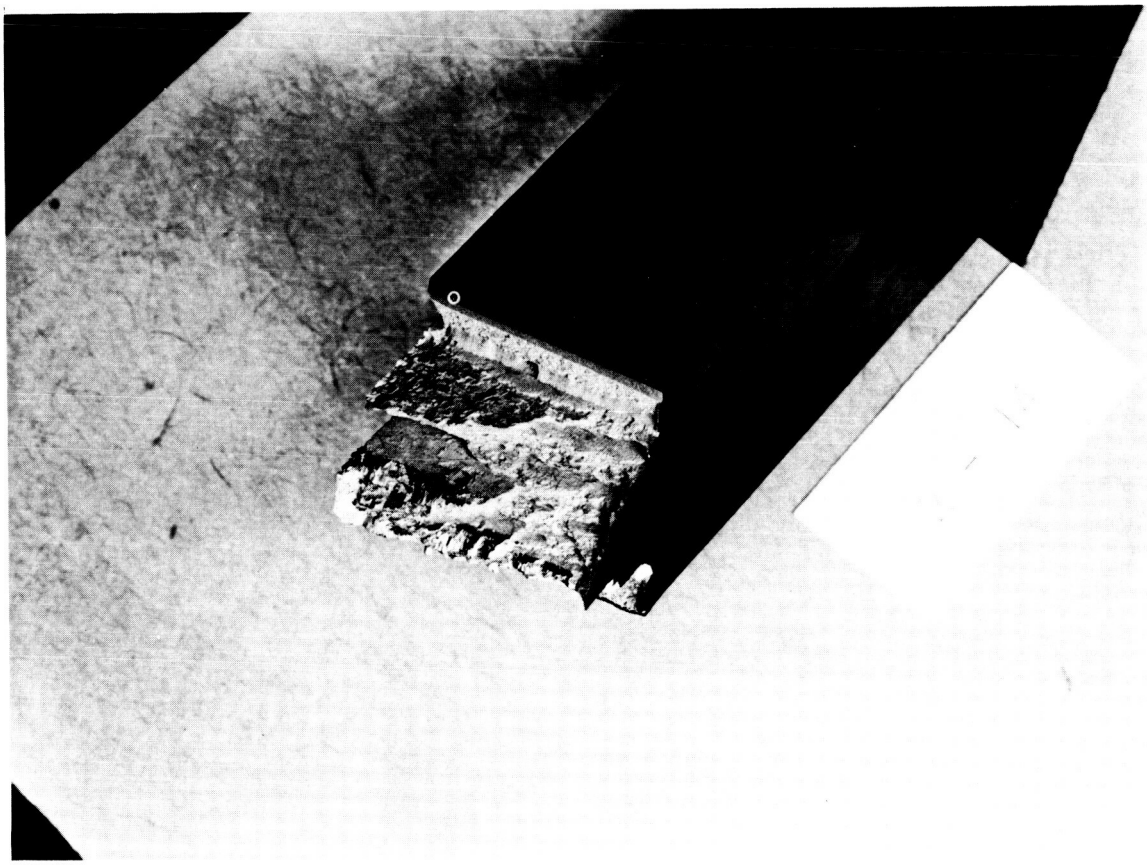

Figure 11.

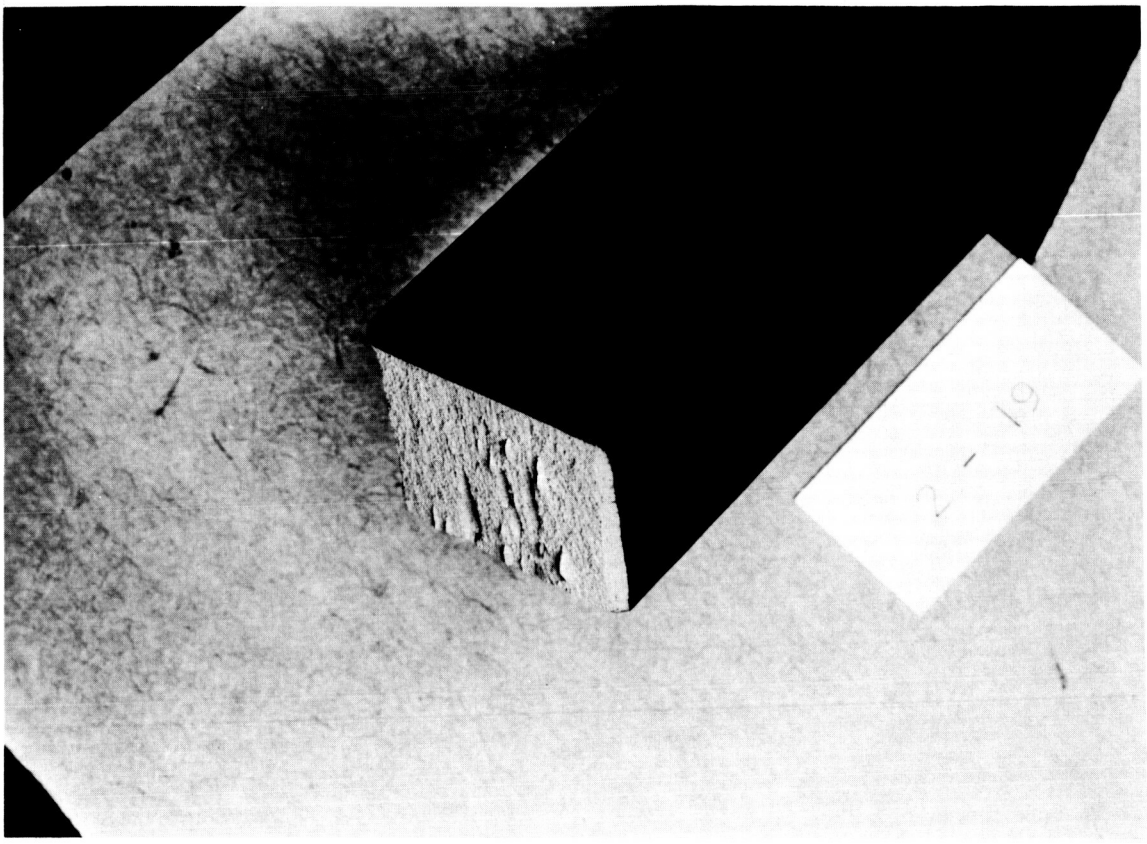

Figure 12.

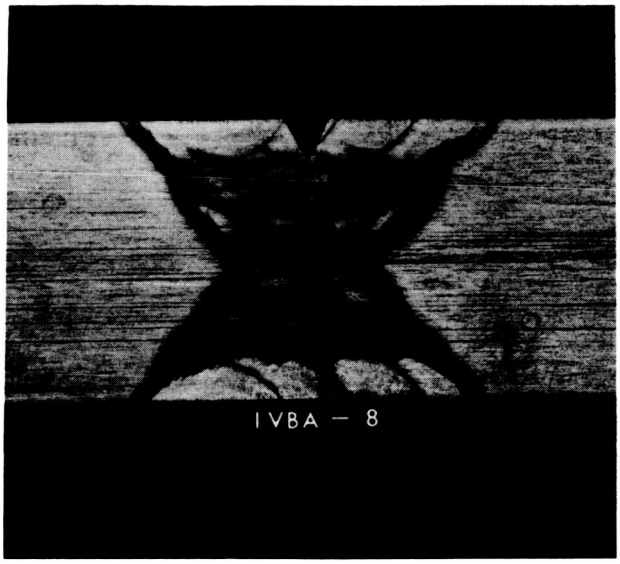

(A) Notch in center of weld

(B) Notch at edge of weld fusion zone fusion zone.

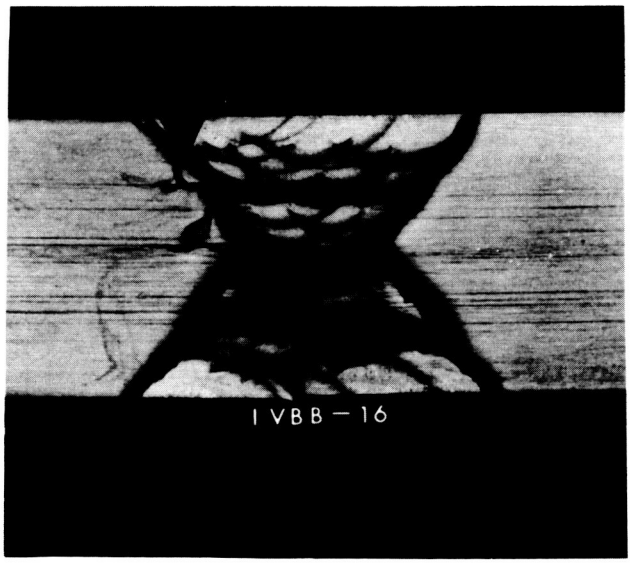

(C) Notch within heat-affected zone

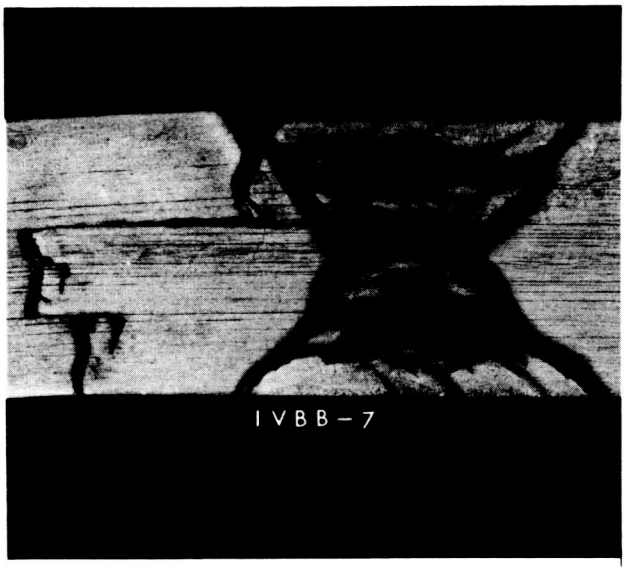

(D) Notch at juncture of heat-affected zone and base metal.

Figure 13a.- Side views of typical bend bars after K_{Ic} tests of TIG weld in plate 2 - 18 Ni (250) maraging steel. Plate cross sections transverse to rolling direction showing different locations of starting notch tipped with fatigue crack. Etched, x2.

Figure 13b.

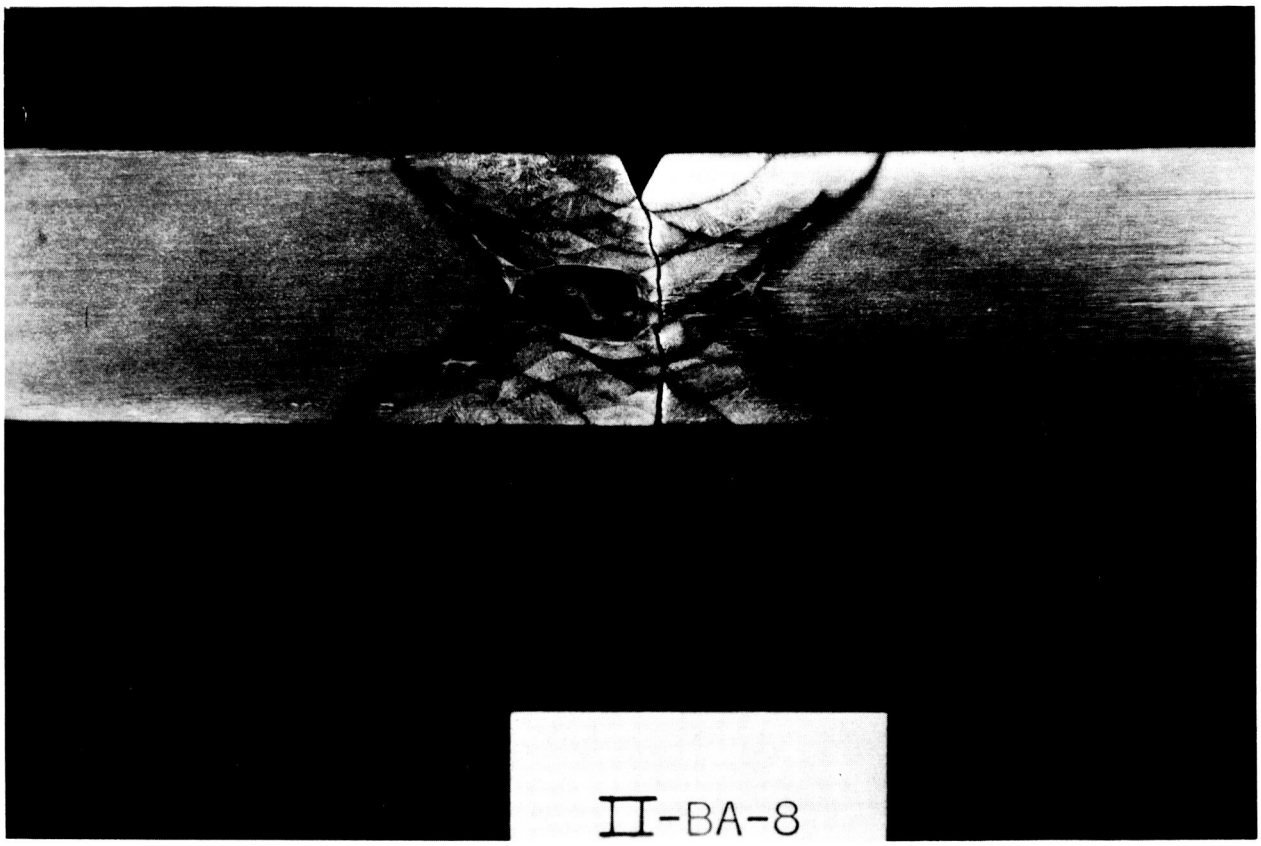

Figure 13b.

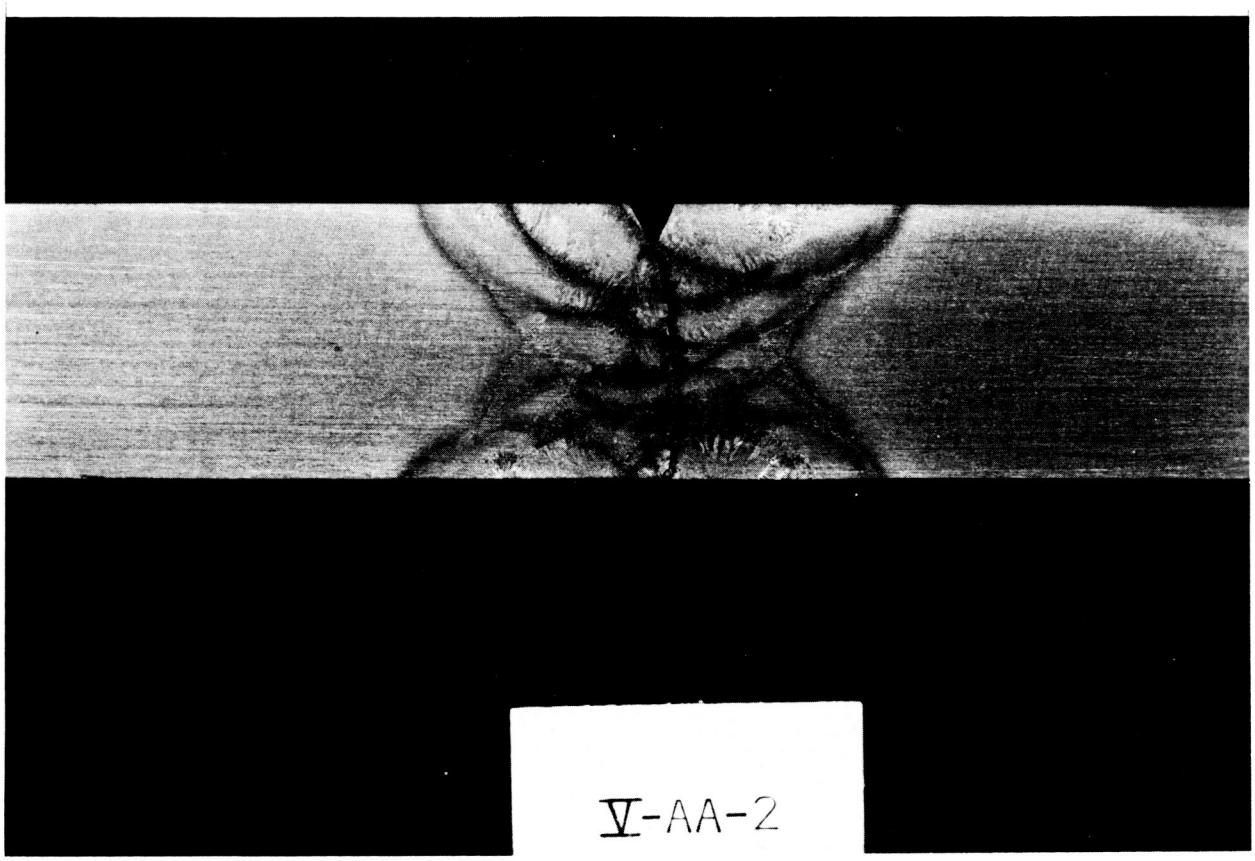

Figure 13c.

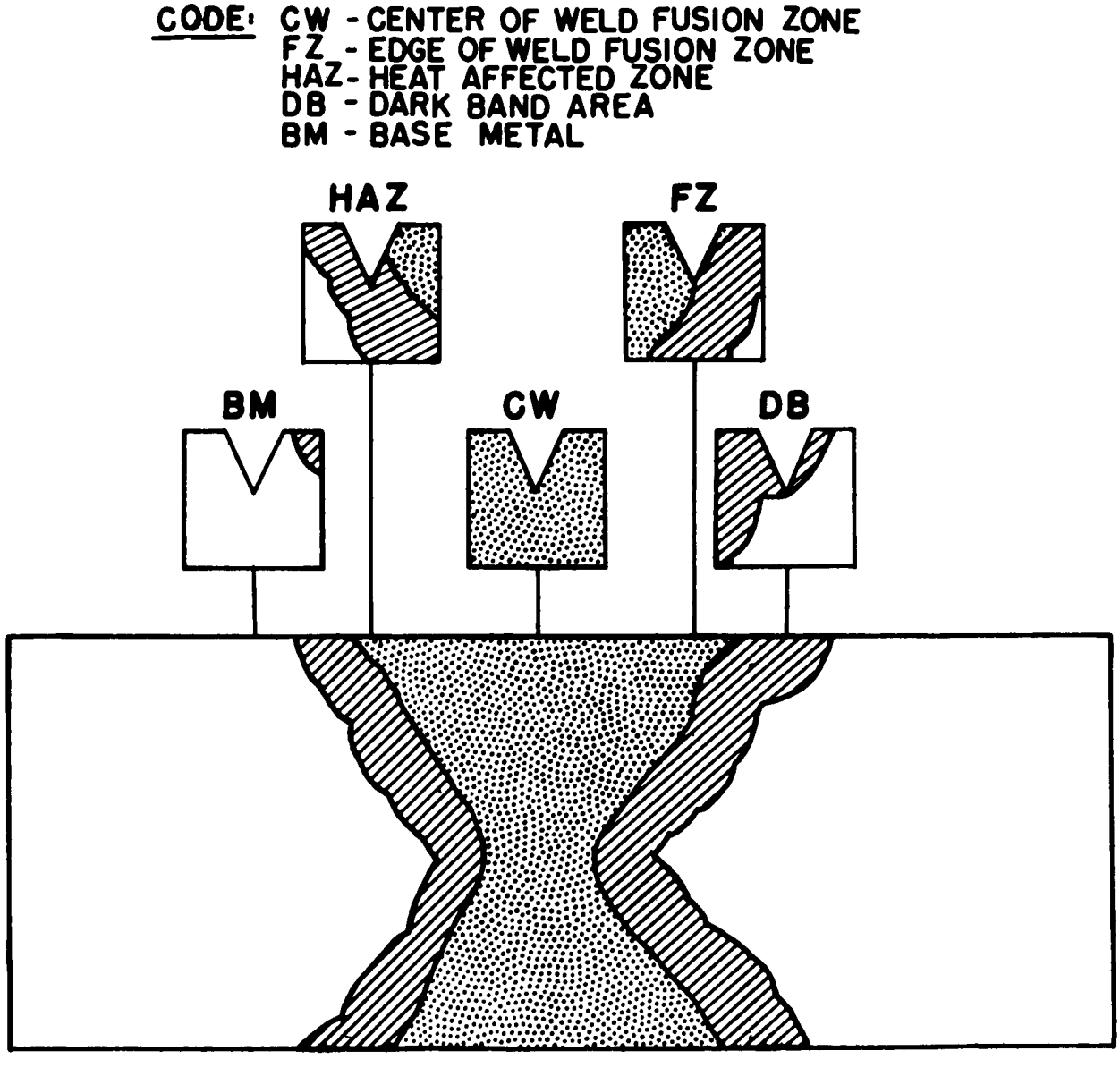

Figure 14.- Cross section of weld area showing different locations of starting notch tipped with fatigue crack.

APPENDIX

Failure Analysis Example - Weld Flaw

Figure A1 shows an enlarged view of a fracture origin in a 156-inch diameter test chamber made of H-11 steel. The prior crack was heat colored and presumably occurred during welding. It was situated at the edge of a longitudinal weld in the cylindrical section. At hydrotest failure (early in 1964) the hoop stress was 77,000 psi. The prior crack was not a very perfect semiellipse and the bottom of the prior crack was poorly delineated. The following data and conclusions illustrate a rather typical situation. Many similar hydrotest failures were encountered in the Polaris steel motor case development program.

Flaw depth "a" = $0.130 \begin{smallmatrix} + .020 \\ - 0 \end{smallmatrix}$ inch

Plate thickness $t = B = 0.38$ inch

$2c = L$ = prior crack length at the surface
$= 0.500$ inch

$$\frac{a}{2c} = 0.260$$

σ_{YS} = uniaxial yield strength = 203,000 psi

$$\frac{\sigma_{hoop}}{\sigma_{YS}} = 0.378$$

$$Q = \left[\Phi^2 - .212\left(\frac{\sigma}{\sigma_{YS}}\right)^2\right] = 1.45 \text{ by the Tiffany chart.}$$

$$K_{Ic}^2 = \frac{3.77\ (77000)^2\ (0.13)}{1.45}$$

$$K_{Ic} \cong 45 \text{ Ksi} \sqrt{\text{in}}.$$

This is the indicated value of K_{Ic} if instability or pop-in occurred at "a" = 0.130. This low value is not uncommon in and near welds in H-11 steel of this thickness.

There is no proof that instability really occurred at "a" = 0.130. It is conceivable that some slow growth extended the crack deeper. If the slow extension had carried the crack all the way through the thickness, the length of the crack would have been $2a_c \cong 1.0$ inch as judged from the photograph. Uncertainty in this number seems to be ±15% and is quite subjective. The fracture still contains almost no shear lip so that K_{Ic} is still the determining toughness for possible arrest. For the through crack: -

$$K_{Ic}^2 = \frac{\pi\ \sigma^2\ a_c}{1 - 0.5\left(\frac{\sigma}{\sigma_{YS}}\right)^2}$$

$$K_{Ic} \cong 100 \text{ Ksi} \sqrt{\text{in}}.$$

This is higher than we have reason to believe is characteristic of the material.

Conclusions:

1. Instability and hydrotest failure were completely determined before the surface crack had penetrated through the thickness.
2. The K_c for H-11 could not tolerate a 2t or 2B crack even at 77,000 psi hoop stress for $t = B = 0.38$ inch.

3. The crack depth at instability seems to have been at the initial black walled prior crack border but this is not a matter of absolute certainty and depends on subjective judgement of the fracture appearance.

4. We did not have adequate data to predict the K_{Ic} or $a_{crit.}$ for such a crack. A considerable uncertainty in $a_{crit.}$ exists.

5. The important thing here is that the crack should have been detected and repaired. Failure prevention is better than failure analysis.

NRL Chemical Analyses - Center of Weld

		Center of Weld		
Element	Rod	Short Arc	MIG	TIG
C	0.02	0.02	0.02	0.02
Mn	0.03	0.03	0.03	0.03
P	0.004	0.002	0.003	0.004
S	0.005	0.005	0.005	0.005
Si	0.02	0.03	0.04	0.02
Ni	18.24	18.2	18.0	18.0
Mo	4.62	4.60	4.60	4.60
Co	7.90	7.79	8.28	7.67
Ti	0.45	0.43	0.43	0.43
Al	0.09	0.09	0.10	0.11

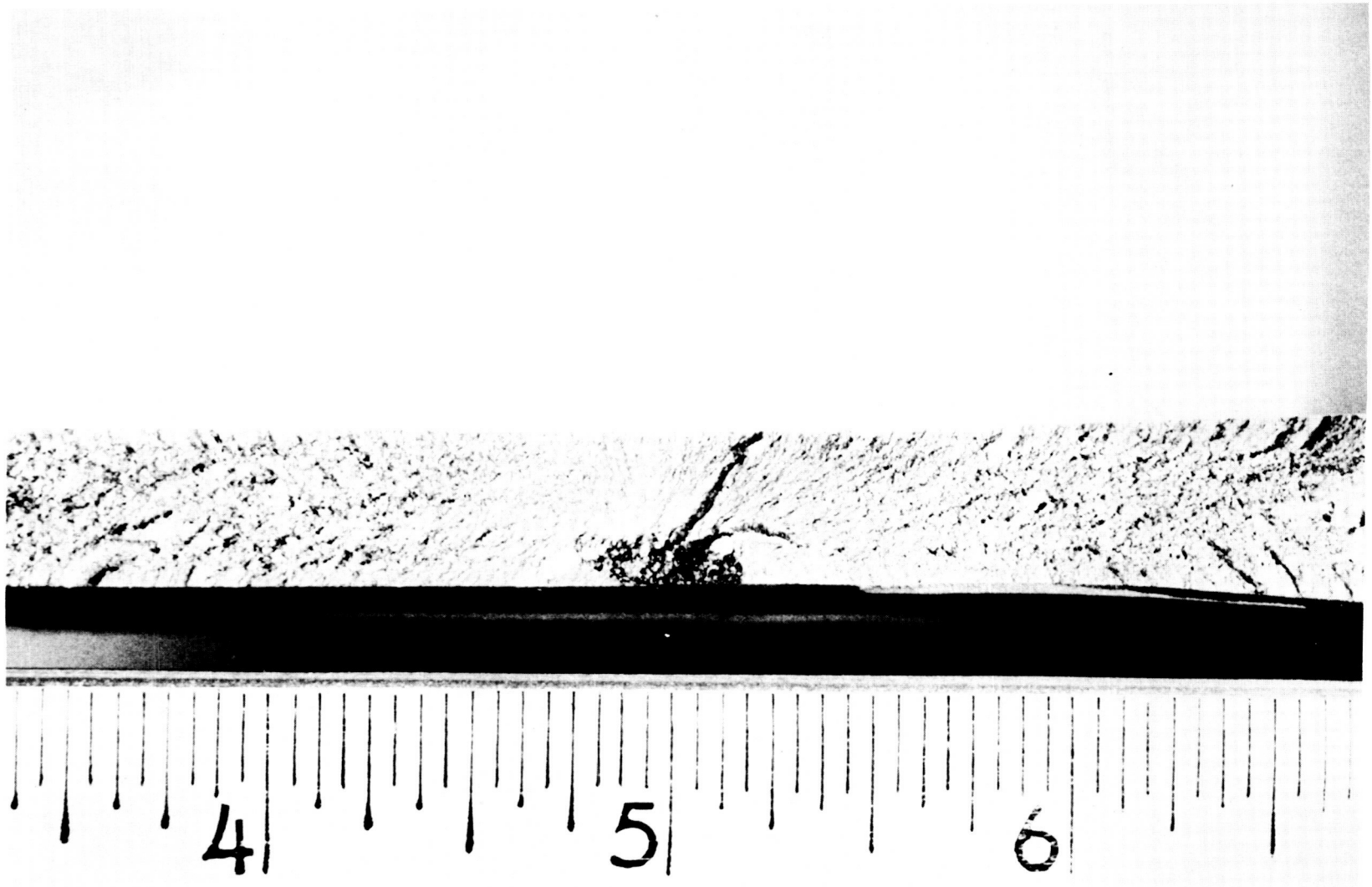

Figure A-1.

Choice of Specimen Type
(3 point bend test)

There are favorable points as well as objectionable points to each type of specimen which one might choose to use in making plane strain fracture toughness measurements. The application in mind will generally dictate one's choice. For the work reported here, it was necessary to evaluate plates with a nominal thickness of 3/4" since the application was the 260" solid booster motor case. Further the material to be evaluated was the 18% Nickel maraging steel which has been subject to a certain amount of banding. It was also desirable to study cracks propagating in the thickness direction (short transverse) as the more likely concern from a practical application standpoint.

Because of the reasons listed here, our choice of specimen was narrowed to either the partially through surface crack in tension or the notch bend test. It was decided that different areas of the weld could be better descriminated using the flat bottom notch of a bend bar rather than the curved perimeter of an elliptical surface notch. It would require from three to four times as much material for a surface notch specimen as that required for a bend specimen.

Three point loading rather than four point loading was selected largely because of convenience. The deflections for a given load are larger in three point loading requiring less magnification of strain measurements. Further one bend test setup is sufficient to test a wide range of specimen sizes in three point loading.

Use of K Values Computed from an Equation

Difficulties not previously experienced were found in this investigation. The problem being austenite segregation and carbide precipitates which result in varying amounts of banding throughout each plate. These variations result in an indeterminate modulus, E. One could avoid this difficulty by notching bend bars in the thickness direction. However, the resulting direction of crack propagation might be unrealistic in relation to the type of failure expected in an actual motor case.

If one measures the compliance, C, of a bend bar as a function of notch depth, the ratio of load to deflection, at the point of interest, determines the effective notch depth for use in calculating $\mathcal{G}$. However, one must know E in order to relate load to crack size. If E is indeterminate the relation of load to crack size is indeterminate. For this reason it was found convenient to represent EC as a function of relative crack depth in equation form and to use this representation and a visual determination of critical notch depth. The resulting K values may scatter and be somewhat altered due to delaminations, but such a procedure establishes a K value for each test which represents a relationship between load and notch depth independent of modulus. Such values are believed to be more useful than the $\mathcal{G}$ values.

NASA-Langley, 1964 CR-140